

PSI-1172/TR-1430

AFOSR-TR-96
0046

GAS PHASE MID-IR LASERS

Reporting Period: 15 November 1992 to 15 November 1995

Final Report

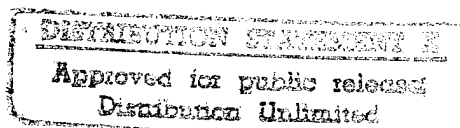
Contract No. F49620-93-C-0004

Prepared by:

Steven J. Davis
William J. Kessler
Karl W. Holtzclaw

Physical Sciences Inc
20 New England Business Center
Andover, MA 01810

January 1996



Prepared for:

Dr. Michael Berman
AFOSR/NC
Directorate of Chemistry & Materials Science
Building 410
Bolling AFB, DC 20332-6448

19960206 073

PSI

PHYSICAL SCIENCES INC.

20 New England Business Center ■ Andover, MA 01810-1077 ■ U.S.A.

DTIC QUALITY INSPECTED 1

REPORT DOCUMENTATION PAGE			Form Approved OMB No. 0704-0188	
Public reporting burden for this collection of information is estimated to average 1 hour per response, including the time for reviewing instructions, searching existing data sources, gathering and maintaining the data needed, and completing and reviewing the collection of information. Send comments regarding this burden estimate or any other aspect of this collection of information, including suggestions for reducing this burden, to Washington Headquarters Services, Directorate for Information Operations and Reports, 1215 Jefferson Davis Highway, Suite 1204, Arlington, VA 22202-4302, and to the Office of Management and Budget, Paperwork Reduction Project (0704-0188), Washington, DC 20503.				
1. AGENCY USE ONLY (Leave blank)	2. REPORT DATE January 1996	3. REPORT TYPE AND DATES COVERED Final Report, 15 November 1992 to 15 November 1995		
4. TITLE AND SUBTITLE Gas Phase Mid-IR Lasers		5. FUNDING NUMBERS 2303/ES 61102F		
6. AUTHOR(S) Steven J. Davis, William J. Kessler and Karl W. Holtzclaw		8. PERFORMING ORGANIZATION REPORT NUMBER PSI-1172/TR 1430		
7. PERFORMING ORGANIZATION NAME(S) AND ADDRESS(ES) Physical Sciences Inc. 20 New England Business Center Andover, MA 01810				
9. SPONSORING/MONITORING AGENCY NAME(S) AND ADDRESS(ES) AFOSR/MENL Directorate of Chemistry & Materials Science Building 410 Bolling AFB, DC 20332-6448 Dr. Berman		10. SPONSORING/MONITORING AGENCY REPORT NUMBER F49620-93-C-0004		
11. SUPPLEMENTARY NOTES				
12a. DISTRIBUTION/AVAILABILITY STATEMENT Approved for public release; distribution unlimited.			12b. DISTRIBUTION CODE	
13. ABSTRACT (Maximum 200 words) A program to develop and apply new mid-IR lasers for Air Force applications is described. Optically pumped lasers that operate either on vibrational or electronic transitions are discussed. Systems include molecular iodine as an electronic transition laser and HF, DF, and HCl as vibrational laser systems. Both experimental and modeling results are described in this report. One of the most exciting aspects of this effort is the possibility of using diode lasers as excitation sources. Finally, efforts to develop miniaturized diagnostics for gas phase species are presented. Applications include new laser development and environmental sensing. Some of this technology has already been transferred to the development of sensors that have been delivered to customers.				
14. SUBJECT TERMS Mid-IR Lasers, Optical Pumping, Diode Lasers, Gas Phase Sensors, Oxygen-Iodine Lasers			15. NUMBER OF PAGES 37	
			16. PRICE CODE	
17. SECURITY CLASSIFICATION OF REPORT Unclassified	18. SECURITY CLASSIFICATION OF THIS PAGE Unclassified	19. SECURITY CLASSIFICATION OF ABSTRACT Unclassified	20. LIMITATION OF ABSTRACT Unlimited	

SECURITY CLASSIFICATION OF THIS PAGE

CLASSIFIED BY:

DECLASSIFY ON:

13. ABSTRACT (Continued)

SECURITY CLASSIFICATION OF THIS PAGE

FINAL REPORT

TITLE: Gas Phase Mid-IR Lasers

PRINCIPAL INVESTIGATOR: Dr. Steven J. Davis

INCLUSIVE DATES: 15 November 1992 to 15 November 1995

CONTRACT NUMBER: F49620-93-C-0004

SENIOR RESEARCH PERSONNEL: Dr. Steven J. Davis, Mr. William J. Kessler, and
Dr. Karl W. Holtzclaw

JUNIOR RESEARCH PERSONNEL: Ms. Amy Wrentmore (Student at Colby College)

PUBLICATIONS and PRESENTATIONS

- a. "Overtone Optically Pumped, mid-IR Lasers," S.J. Davis and W.J. Kessler, Paper at Lasers 93 Meeting, Lake Tahoe, NV, Dec 1993
- b. "Near IR Iodine Laser Based on Diode Pumping," S.J. Davis and W.J. Kessler, Paper at Lasers 93 Meeting, Lake Tahoe, NV, Dec 1993
- c. "Mid-IR Gas Phase Optically Pumped Lasers," S.J. Davis, W.J. Kessler, K.W. Holtzclaw, and C.R. Jones, Paper at 10th International Conference on Gas Flow and Chemical Lasers, Lake Constance, Germany, Aug 1994
- d. "Diode Laser-Based Measurements of Water Vapor and Ground State Oxygen in Chemical Oxygen Iodine Lasers," M.G. Allen, K.L. Carleton, S.J. Davis, W. J. Kessler, and K.R. McManus, 25th AIAA Plasmadynamics and Lasers Conference, Colorado Springs, CO Paper 94-2433 (1994)
- e. "Ultra-sensitive Dual Beam Absorption and Gain Spectroscopy: Applications for Near-IR and Visible Diode Laser Sensors," M.G. Allen, K.L. Carleton, S.J. Davis, W.J. Kessler, C.E. Otis, D.A. Polombo, and D.M. Sonnenfroh, Applied Optics **34**, 3240 1995.
- f. "State-Resolved Rotational Energy Transfer in ICl(B) , ($v = 1$) for $\text{ICl} + \text{ICl}$ Collisions," K.W. Holtzclaw, S.J. Davis, and W.J. Kessler, submitted to Journ. Chem. Phys. (1995)
- g. "Overtone Pumped HCl and HF Lasers," W.J. Kessler, S.J. Davis, G. Hager, and H. Miller. Jour. Appl. Physics (Manuscript in Preparation).

- h. "Small Signal Gain Studies in I_2 Produced by a Low-Power Diode Laser,"
K.W. Holtzclaw and S.J. Davis, Appl. Phys. Lett. (Manuscript in Preparation).
- i. "Room Temperature Diode Lasers: New Tools for Applied and Basic Research,"
S.J. Davis, Lasers 95, Invited Paper, Charleston, SC (1995)

Contents

	<u>Page</u>
Figures	iv
Summary	1
1. Introduction	2
2. Molecular Iodine Laser	4
3. Feedback Control for Linelocking Pump Laser to Absorption Line	8
4. Optically Pumped HF and HCl Lasers	11
5. HCl Laser Experiments	14
6. Alexandrite Laser Pumped DF and HCl Lasers	17
6.1 DF Laser Experiments	17
6.2 Alexandrite Laser Pumped HCl Laser	18
7. Design of Diode Laser Pumped HF Laser	22
8. Applications of Diode Laser Based Sensors	25
8.1 Preliminary Determination of Linestrength of Water Absorption Line Near 1.39 μm	27
8.2 Water Vapor Sensor Development	28
8.3 Description of Ultra-Sensitive Absorption Measurements	29
8.4 Development and Testing of Diode Oxygen Sensor for COIL	30
8.5 Demonstration of Gain on the I_2 (B \rightarrow X) System Produced by a Low Power Diode Laser	31
8.6 Experiment	32
9. Conclusions	36
10. References	37

List of Figures

<u>Figure No.</u>	<u>Page</u>
1	Two Methods for Producing Mid-IR, Optically Pumped Tunable Lasers 3
2	Block Diagram of Molecular Iodine Laser Pumped by Diode Laser Pumped Frequency Doubled Nd:YAG Laser 4
3	Excitation Spectrum Obtained by Scanning the Nd:YAG Laser Through Three Molecular Iodine Absorption Lines. 5
4	Excitation and Laser Cycles for Nd:YAG Pumped Laser 5
5	Excitation Spectra Demonstrating Both Broadband I ₂ Laser Output and Spontaneous Side Fluorescence. 6
6	Output Power of I ₂ Laser as Function of Nd:YAG Laser Power 7
7	Block Diagram of Closed Loop Controller 8
8	Control of Iodine LIF Intensity Through Laser Wavelength Modulator of the Pump Laser 9
9	I ₂ Cell Intensity and Control Voltage Versus Time for 9-h Control Experiment 10
10	Percent Difference Between Control Setpoint and I ₂ Cell Output Intensity Versus Time for 9-h Control Experiment 10
11	Block Diagram of HF Laser Apparatus 11
12	Excitation Spectrum of HF Laser Output as Excitation Wavelength Was Varied. 12
13	Configuration for Side-Pumped HF Laser 12
14	Dependence of HF Laser Output Power on HF Pressure for Side-Pumped Configuration 13
15	Experimental Arrangement for the OPO-Pumped HCl Experiments 14
16	Excitation Spectrum of Several Lines in the (2,0) Band of HCl. 15

List of Figures (continued)

<u>Figure No.</u>		<u>Page</u>
17	Spectrally Resolved HCl Laser Output Resulting from Excitation of the $J' = 2$ Level Within $v' = 2..$	15
18	Block Diagram of Alexandrite Pumped DF Laser	18
19	Laser Excitation Spectrum of the DF (3,0) Laser	19
20	Spectrally Resolved DF Laser Emission From Alexandrite-Pumped DF Laser	19
21	Laser Excitation Spectrum of HCl(J4) Line on the (3,0) Band Obtained Using High Power, Narrow Band, Raman-Shifted Alexandrite Laser	20
22	Linewidth of the LIF from HCl(J4) $v=3$ as a Function of the HCl Concentration	21
23	Predicted Optical Gain in DF for 1 Watt Pumped Power and a DF Number Density of Approximately 2 Torr	22
24	Predictions of Small Signal Gain Coefficient Using Resonant Cavity Pumping.	23
25	Laser Excitation Spectrum for HF(2,0) LIF as Diode Laser is Scanned Over the P Line.	24
26	Layout for Typical Diode Laser Sensor	25
27	Absorption Spectrum of ($^2P_{1/2} - ^2P_{3/2}$) Line in Atomic Iodine Obtained at a Temperature of 1050 K.	26
28	Absorption Spectrum of Atomic Iodine Near 1.315 μm Obtained With Tunable Diode Laser.	26
29	Curve of Growth For Water Vapor Absorption on the 1.39235 μm Line vs Predictions of HITRAN	27
30	Evolution of Water Vapor From During a COIL Run	28
31	Schematic of Balanced Radiometric Detector System	29

List of Figures (continued)

<u>Figure No.</u>		<u>Page</u>
32	Data From RADICL Test at Phillips Lab.	31
33	Experimental Arrangement for Demonstration of Pumping of $I_2(B)$ by a Low Power Diode Laser	32
34	Absorption From Ground State Iodine	33
35	Pump/Probe Scheme Used in This Experiment	34
36	Diode Laser Scan Showing Gain Produced Over Narrow Frequency Interval	35
37	Expanded View of the P(38) Line Showing Gain Within the Doppler Width of the Absorption Transition	35

SUMMARY

In this report we have described results of a multi-faceted program that investigated the production and some applications of near IR lasers. It is quite clear from the results of this effort that the hydrogen halides have considerable potential for development into high power, discretely tunable, near IR laser systems. We demonstrated laser output from HF, HCl, and DF spanning the spectral range of 2.7 to nearly 4 microns. In addition, these systems show promise for direct diode laser pumping.

We have also developed several sensors for various applications including the chemical oxygen iodine laser (COIL). Using room temperature, tunable diode lasers we have demonstrated sensitive detection of H_2O , I atoms, and ground state O_2 . Under separate funding, the initial studies supported by AFOSR were extended to the development of fieldable sensors that have been tested on the Phillips Lab RADICL device.

Finally we also demonstrated the production of optical gain in molecular iodine when pumped by a miniature diode laser. This development has significant implications for future work because it not only proved that diode lasers can pump single spectral lines in gas phase species, but it also demonstrated an ultra-sensitive gain diagnostic that will have numerous future important applications.

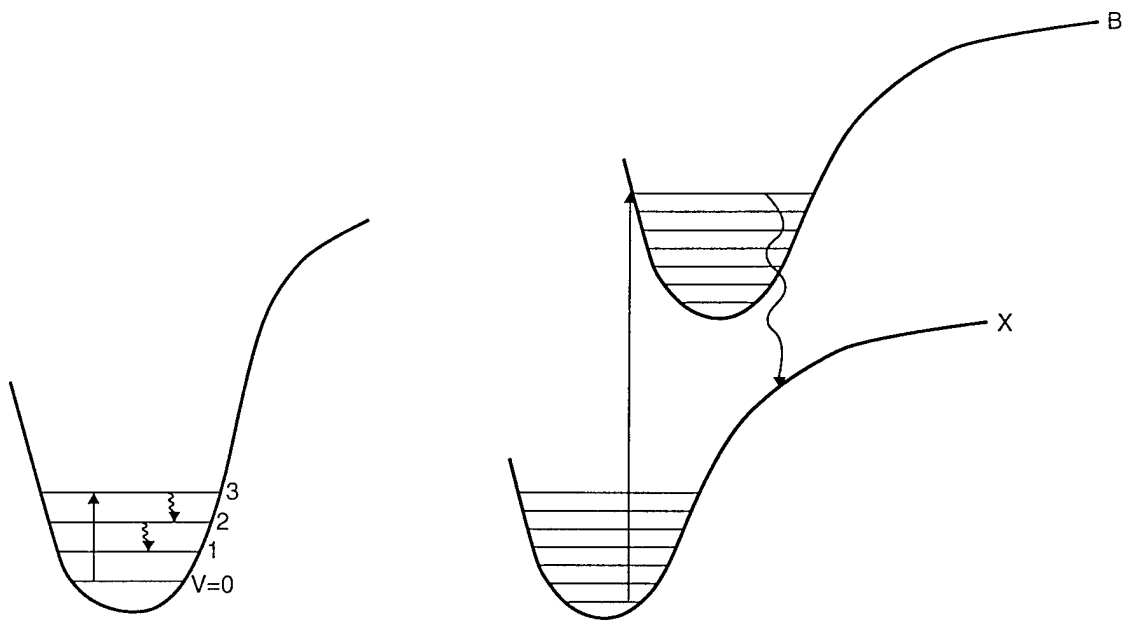
1. INTRODUCTION

The objective of this project is to investigate the concept of producing and applying efficient mid-IR lasers based on optical pumping of simple diatomic molecules. We are examining vibrational lasers of hydrogen halide molecules and excitation of electronic states of halogen molecules as candidate systems. We are developing a comprehensive analytical model to interpret data from our laser studies and to guide the development of new candidate systems. In addition, we are also developing novel uses for miniature, room temperature diode lasers as diagnostics for COIL and other laser systems. These diode lasers also have significant applications as sensors for environmental pollutants of Air Force interest such as HF and HCl. Several projects were completed during this effort and we describe them in detail below. The topics are covered sequentially.

During this program, we completed several projects:

- Development and characterization of a molecular iodine laser powered by a miniature diode pumped Nd:YAG laser.
- Design and demonstration of several mid-IR lasers based on hydrogen halide overtone pumping.
- Design of diode laser pumped HF laser.
- Development of diode laser based gas phase sensors for COIL.
- Design and demonstration of an HCl mid IR laser pumped by a Raman-shifted alexandrite laser. We have frequency locked the alexandrite laser to a single frequency tunable diode laser. We have also used the alexandrite laser to measure the self broadening coefficient of the HCl(3,0) overtone transition.
- Development and demonstration of a diode laser sensor for the concentration of ground state oxygen for COIL. This device was field tested at Phillips Lab on the RADICL device.
- Demonstration of diode pumped gas phase amplifier.

We investigated two methods for producing mid-IR laser production: overtone pumping of vibrational levels in hydrogen halides and excitation of electronic levels in halogen molecules. These two approaches are illustrated in Figure 1. Several hydrogen halide species were investigated including: HF, HCl, and DF. With respect to electronic excitation, we have been studying I₂ as a prototype system. A molecular iodine laser pumped by a miniature diode laser pumped, frequency-doubled Nd:YAG laser was also demonstrated. Direct diode laser pumping of gases was also studied, and gain was produced in I₂. Finally we extended the diode laser based work to the development of miniature sensors for the chemical oxygen iodine laser (COIL).

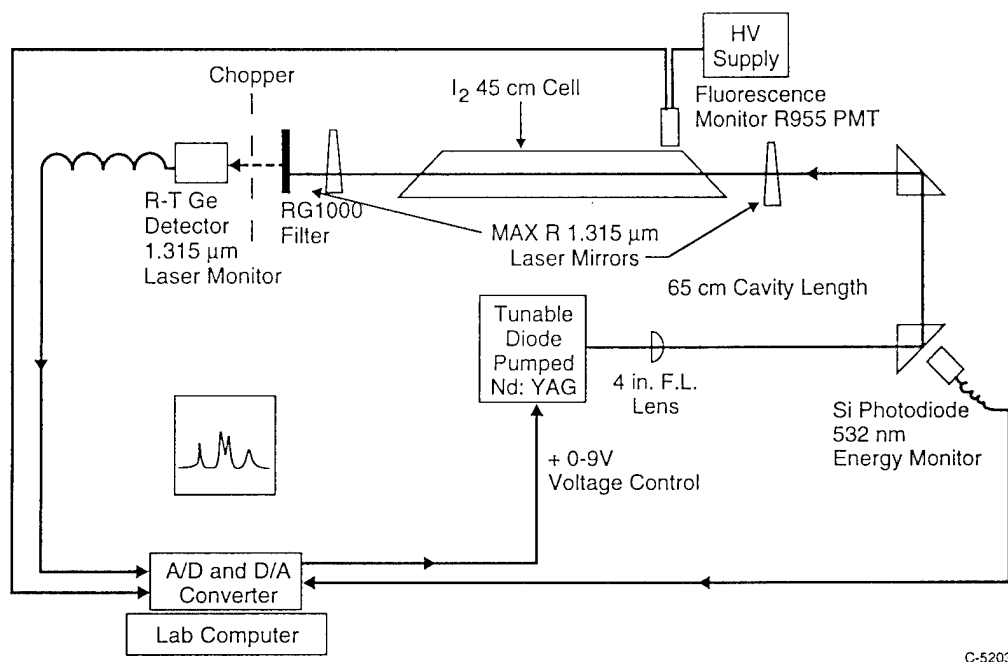


C-5201

Figure 1
Two Methods for Producing Mid-IR, Optically Pumped Tunable Lasers

2. MOLECULAR IODINE LASER

The B - X system in molecular iodine provides a valuable prototype electronic transition laser system for investigation. Although the long wavelength limit of the I_2 system is only $1.34\text{ }\mu\text{m}$, other analogous systems such as molecular bromine will provide laser output to beyond $3\text{ }\mu\text{m}$. In addition, the iodine system can be used to test optical pumping schemes that can be applied to other systems.^{1,2} For example, one important potential excitation scheme involves diode lasers. In this respect we can investigate both direct diode laser pumping and diode laser pumped lasers as excitation sources. In our last report we presented preliminary results in which we used a miniature diode pumped Nd:YAG laser to pump an I_2 laser. The basic experiment is shown in Figure 2.



C-5203

Figure 2
Block Diagram of Molecular Iodine Laser
Pumped by Diode Laser Pumped Frequency Doubled Nd:YAG Laser

The excitation source was a Lightwave Electronics Model 140 Nd:YAG laser pumped by a diode laser. This miniature Nd:YAG laser ($6 \times 6 \times 10\text{ cm}$) produces 300 mW at the $1.06\text{ }\mu\text{m}$ fundamental and 105 mW frequency doubled at 532 nm . The laser is tunable over 1 cm^{-1} , via a temperature-controlled frequency doubling crystal and can be brought into resonance with several iodine absorption lines. In Figure 3, we show an excitation spectrum as a function of the frequency of the diode pumped Nd:YAG laser. Three strong absorption peaks are apparent in Figure 3.

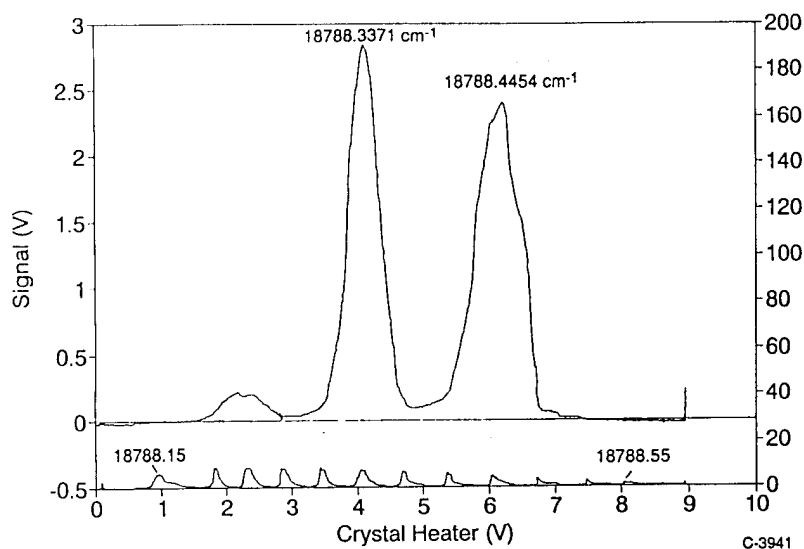


Figure 3

Excitation Spectrum Obtained by Scanning the Nd:YAG Laser Through Three Molecular Iodine Absorption Lines. The Observed Signal is Due to Spontaneous Side Fluorescence.

The frequency markers in Figure 3 were obtained by passing a portion of the Nd:YAG laser beam through a Fabry-Perot (F-P) interferometer with a fixed mirror spacing. The markers represent consecutive transmission orders of the interferometer, and their separation is determined by the F-P mirror spacing. These markers provide an accurate frequency scale.

We obtained laser oscillation from the optically excited iodine medium. The output wavelengths covered the wavelength range of approximately 700 to 1340 nm. The excitation and laser cycles are indicated in Figure 4. Note that the B - X system in molecular iodine provides a wide tuning range in emission.

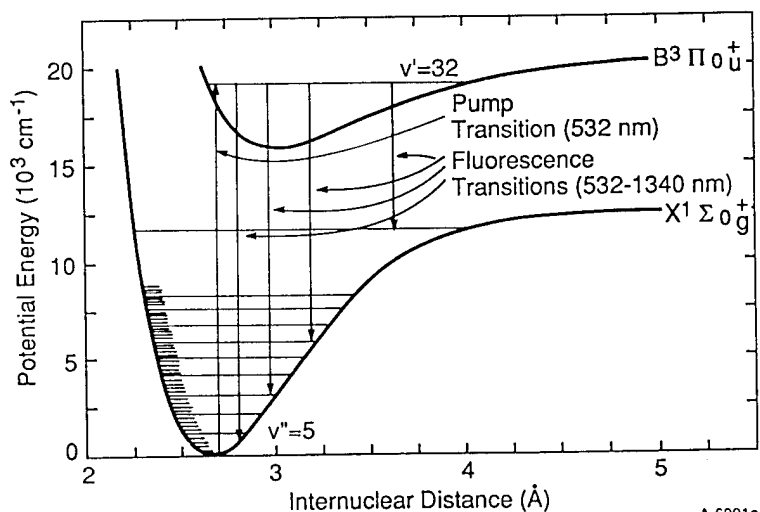


Figure 4

Excitation and Laser Cycles for Nd:YAG Pumped Laser

In Figure 5, we present data that compares spontaneous side fluorescence and iodine laser output as a function of the excitation frequency. The side fluorescence appears as a spectrally broad line, while the iodine laser output appears as a series of sharp features. These groupings of lines are actually due to hyperfine structure in the I_2 species. Since the iodine laser was run just above threshold, laser oscillation occurs only when the frequency of the Nd:YAG laser is near the center frequency of one of the many hyperfine transitions in the iodine (B - X) system. The broad side fluorescence is due to Doppler broadening of the hyperfine transitions. This "hyperfine broadening" is well known in iodine.^{3,4} In previous work, we described this behavior in optically pumped lasers in detail.¹

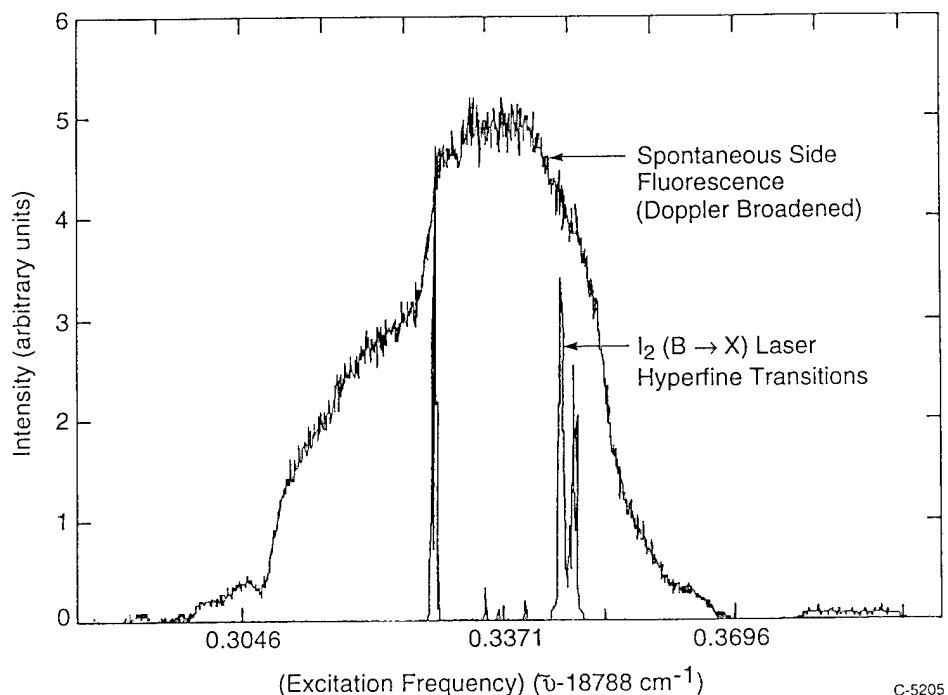


Figure 5
Excitation Spectra Demonstrating Both Broadband I_2 Laser Output and Spontaneous Side Fluorescence. See Text for Explanation.

Figure 6 shows the output power of the iodine laser as a function of the power of the Nd:YAG laser incident on the cell. Other similar data indicated a threshold of only 12 mW of pump power. We also measured a conversion efficiency of greater than 1% which is nearly two orders of magnitude higher than for iodine lasers pumped by argon ion lasers.² This is an encouraging result and demonstrates that diode pumped systems can be used as efficient pump sources for gas phase optically excited lasers.

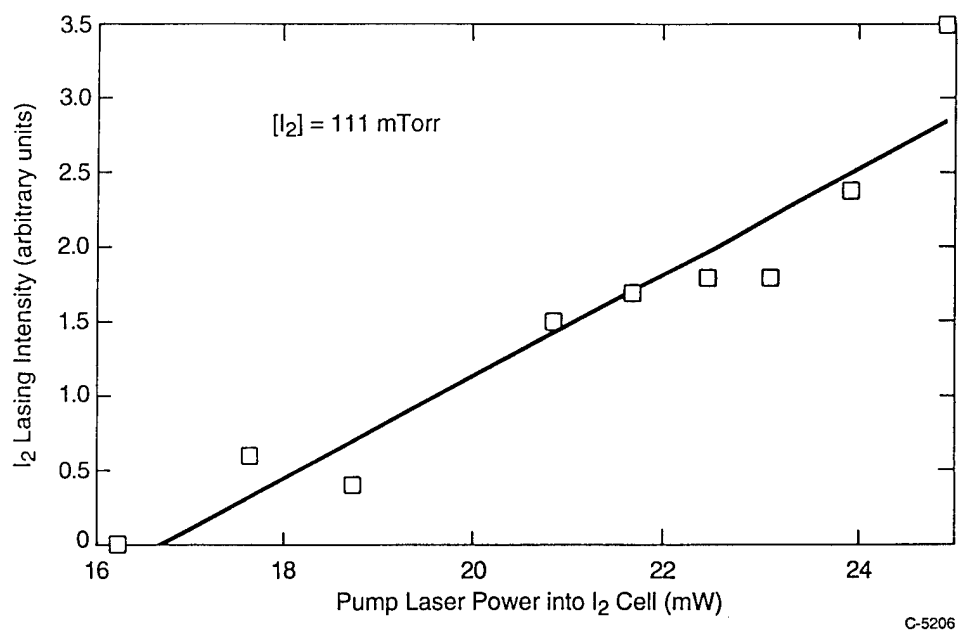


Figure 6
Output Power of I_2 Laser as Function of Nd:YAG Laser Power

3. FEEDBACK CONTROL FOR LINELOCKING PUMP LASER TO ABSORPTION LINE

Coupling of the pump laser to the medium is one of the issues crucial to the efficient operation of any optically pumped molecular laser. It depends upon fundamental molecular parameters such as the absorption line width and the absorption cross section. Exact tuning of a pump laser to an absorption line is required. In addition, one must be able to lock the frequency of the pump laser to the absorption line in order to assure that the excitation is at the correct wavelength. We have developed a closed loop controller to lock a pump laser such as a diode laser to a molecular absorption line. In particular, we have demonstrated this controller on a tunable Nd:YAG laser that is used to pump the molecular iodine laser.

As indicated above, this laser can tune over several iodine absorption lines on the B - X system of I_2 . The slight asymmetry in the fluorescence lines shown in Figure 3 is due to the hyperfine structure in the I_2 molecule (nuclear spin $I = 5/2$). The ability of the narrow band ($\Delta\nu < 100$ MHz) laser to tune over the absorption line forms the basis of the frequency controller as described below.

A block diagram of the controller is shown in Figure 7 and consists of a Si photodiode to monitor the iodine LIF emission intensity and a controller which processes the LIF intensity from the sensor and in turn supplies an output signal to an actuator affecting the LIF intensity. The control actuator relies on the dependence of the LIF on the overlap integral between the I_2 absorption line and the pump laser emission line. The LIF intensity is controlled by tuning the laser output wavelength nearer to, or farther away from the absorption linecenter. A schematic diagram depicting this relationship is shown in Figure 8.

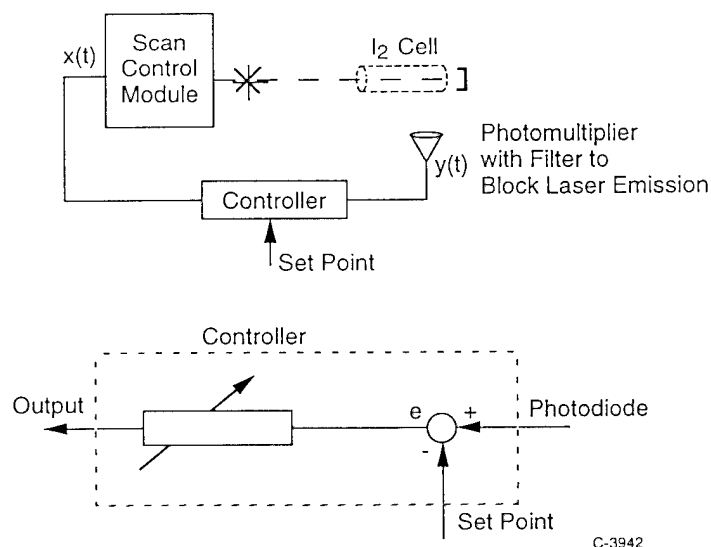


Figure 7
Block Diagram of Closed Loop Controller

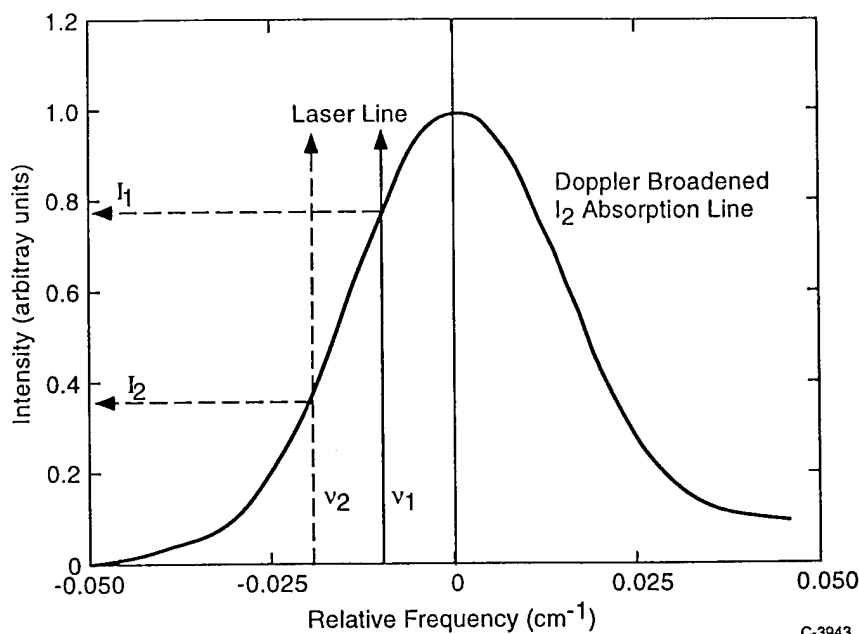


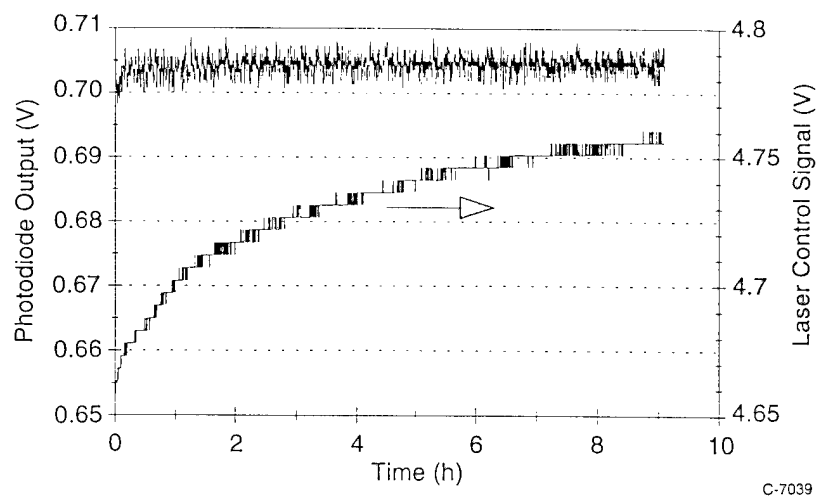
Figure 8

Control of Iodine LIF Intensity Through Laser Wavelength Modulator of the Pump Laser

This control scheme was tested using the miniature diode laser pumped Nd:YAG laser as the I₂ optical pump source. The control algorithm was implemented using a laboratory PC enabling A/D and D/A conversion. The output function for the integral controller may be written as follows:

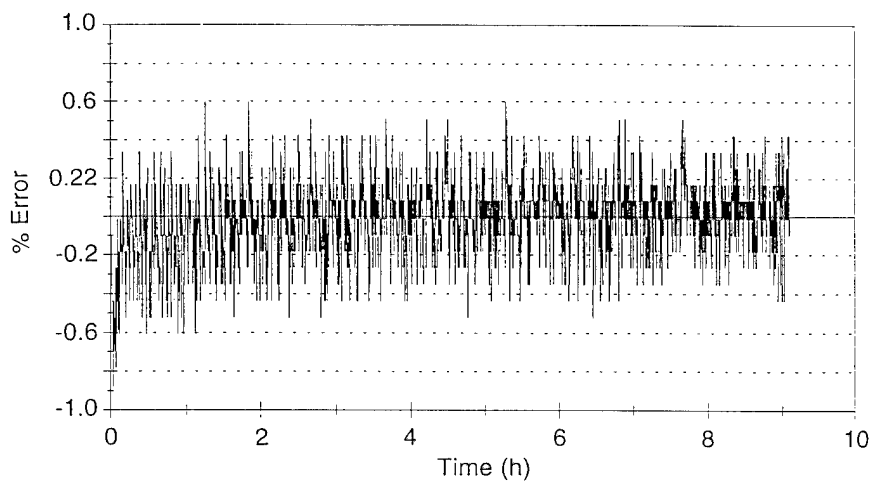
$$y(t) = I \int_0^{\tau} e(t)dt \quad (1)$$

where I is a constant gain coefficient, e(t) is an error term representing the difference between the measured I₂ LIF output intensity, x(t), and a user supplied setpoint value, s (i.e., e(t) = s-x(t)). This functional form was chosen in order to facilitate compensation for low-frequency drift in the scan control offset. Figure 9 shows a time trace representing the iodine LIF output intensity with the controller on. Both the voltage supplied to the doubling crystal and the LIF intensity are presented. This example demonstrates the effectiveness of the integral controller in maintaining a constant lamp output intensity. An expanded view of the LIF output is presented in Figure 10. Over the 9-h period, the rms variation was only 0.12%. Clearly the laser was locked to the absorption line using this simple closed loop controller. This strategy is also applicable to any tunable pump lasers including diode lasers.



C-7039

Figure 9
 I_2 Cell Intensity and Control Voltage Versus Time for 9-h Control Experiment



C-7040

Figure 10
 Percent Difference Between the Control Setpoint and
 I_2 Cell Output Intensity Versus Time for a 9-h Control Experiment

4. OPTICALLY PUMPED HF AND HCl LASERS

In order to demonstrate some of the attractive features of optically pumped hydrogen halide laser systems, we designed and conducted several experiments using HF and HCl as the laser species. The HF experiments were performed at PSI using a Raman-shifted pulsed dye laser as the excitation source. The apparatus is indicated in Figure 11. The dye laser was pumped by a 581 Quantel Nd:YAG laser that was frequency doubled. This laser produced 10 ns, 532 nm laser pulses containing approximately 450 mJ. The dye laser linewidth was less than 0.2 cm^{-1} . We used a rhodamine 640/DCM dye mixture to produce output energies of 75 mJ at 620 nm. A hydrogen Raman shifter produced approximately 2 mJ near 1300 nm, exciting several rotational levels in the (2,0) band of HF.

As shown in Figure 11, we used several diagnostics: a filtered InSb detector to monitor broadband HF laser output and a monochromator to disperse the HF laser output.

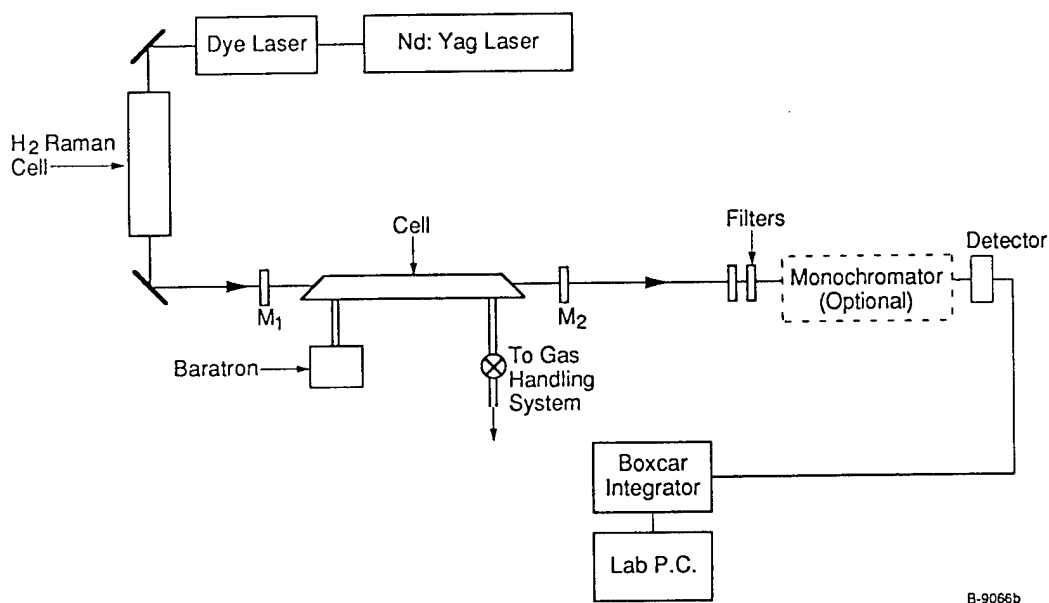


Figure 11
Block Diagram of HF Laser Apparatus

We also used a Stanford Research Instruments boxcar integrator to signal average several pulses in order to obtain excitation spectra. In Figure 12, we show an excitation spectrum in which the broadband HF laser output was monitored as the excitation wavelength was varied. Several HF rovibrational lines are indicated.

We conducted several other experiments on HF including a side pumped configuration that is shown in Figure 13. This system imitates the geometry that might be used in a diode pumped

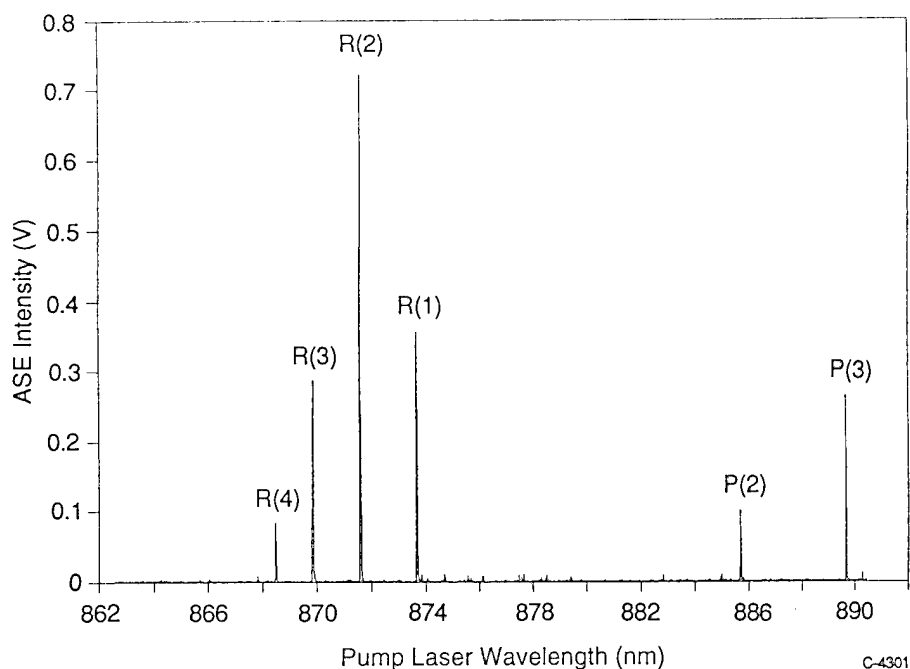


Figure 12
Excitation Spectrum of HF Laser Output as Excitation Wavelength Was Varied.
For These Data, the (3,0) Band Was Excited.

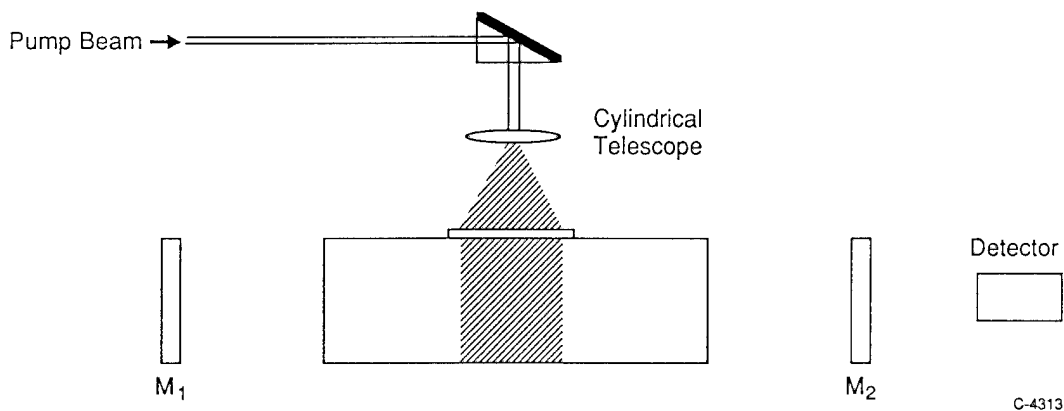


Figure 13
Configuration for Side-Pumped HF Laser

laser system such as used in side pumped solid state lasers. For these experiments we used a cylindrical telescope to focus the Raman-shifted dye laser into a ribbon approximately 2 cm wide and 2 mm thick. We observed laser oscillation over an extended pressure range of HF as shown in Figure 14. Using this side pumped configuration and short (10 ns) pulse pumping, quenching by HF is not a significant kinetic process.

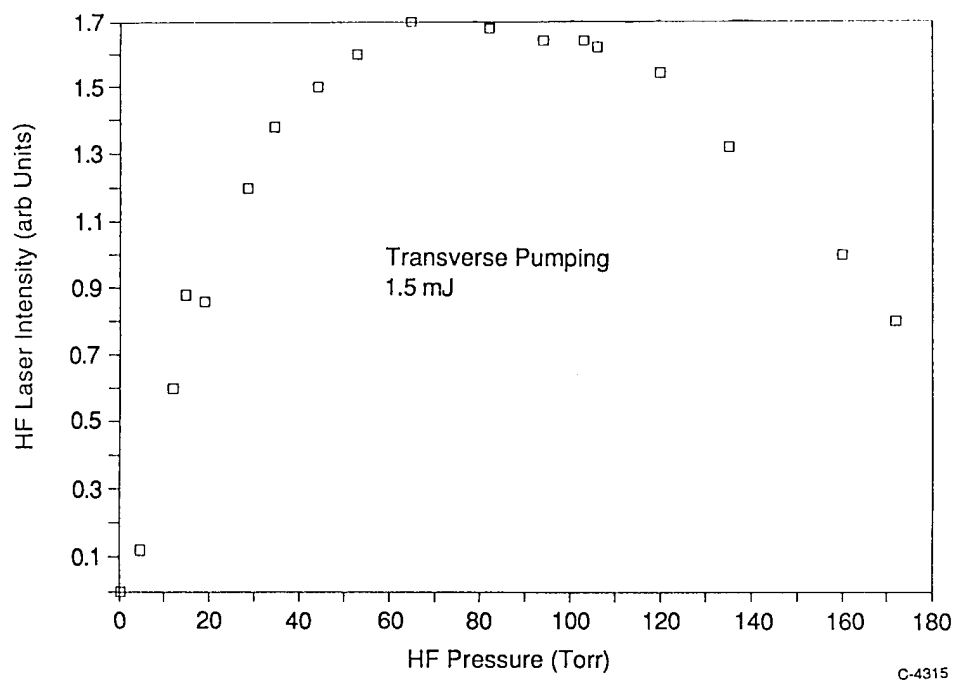


Figure 14
Dependence of HF Laser Output Power on HF Pressure for Side-Pumped Configuration

5. HCl LASER EXPERIMENTS

Through a collaborative effort with Phillips Laboratory, we completed a study of an optically pumped HCl laser. For this investigation, W. J. Kessler, of PSI, worked at Phillips Laboratory with Dr. H. Miller. We chose this approach to utilize the Phillips Laboratory optical parametric oscillator (OPO) that provided the appropriate output wavelengths to pump HCl lines within the (2,0) band near $1.7\ \mu\text{m}$. The apparatus for these experiments are indicated in Figure 15. The heart of this setup was the Spectra Technologies STI Mirage 3000 OPO that provided several mJ with linewidths on the order of 500 MHz. The diagnostics and gas handling facilities were similar to those described above.

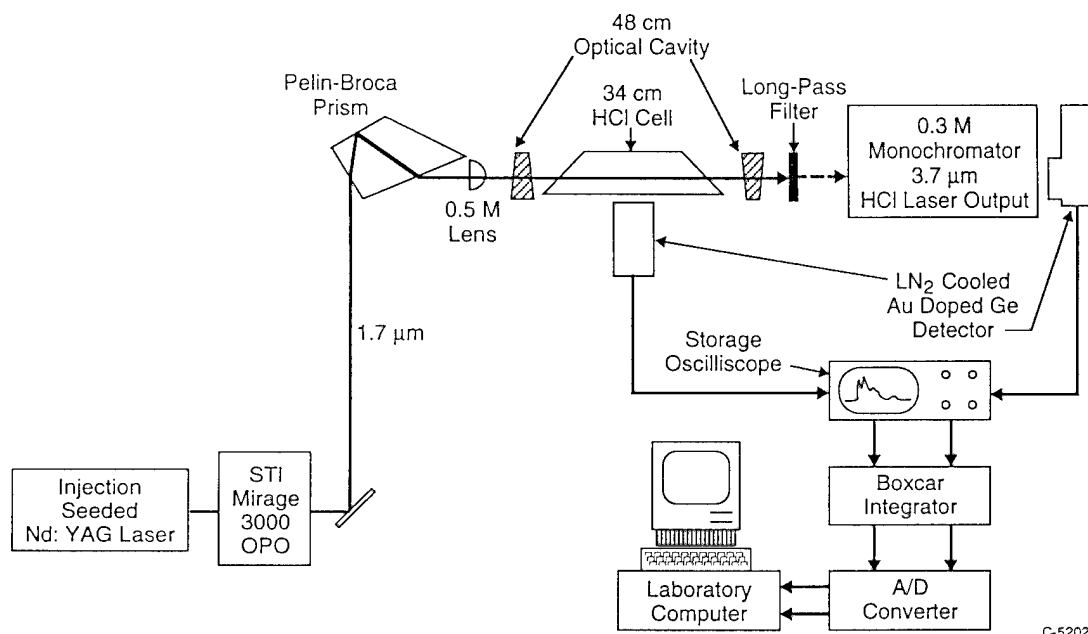


Figure 15
Experimental Arrangement for the OPO-Pumped HCl Experiments

In Figure 16, we present excitation spectra for the HCl laser; the two chlorine isotopes give rise to pairs of HCl lines as indicated in the data.

Spectrally resolved HCl laser spectra yielded information concerning the rovibrational lines that participated in the lasing process. Sample data resulting from excitation of the R(2) line are shown in Figure 17. Laser oscillation is observed from several J' levels: $J' = 0, 1, 2$, and 3 . This demonstrates the dominant role of rotational relaxation in the optically pumped $v' = 2$ level. Indeed, rotational relaxation is the fastest kinetic process within the optically pumped level. It does not necessarily degrade the performance of the laser since many of the collisionally populated levels participate in the laser output.

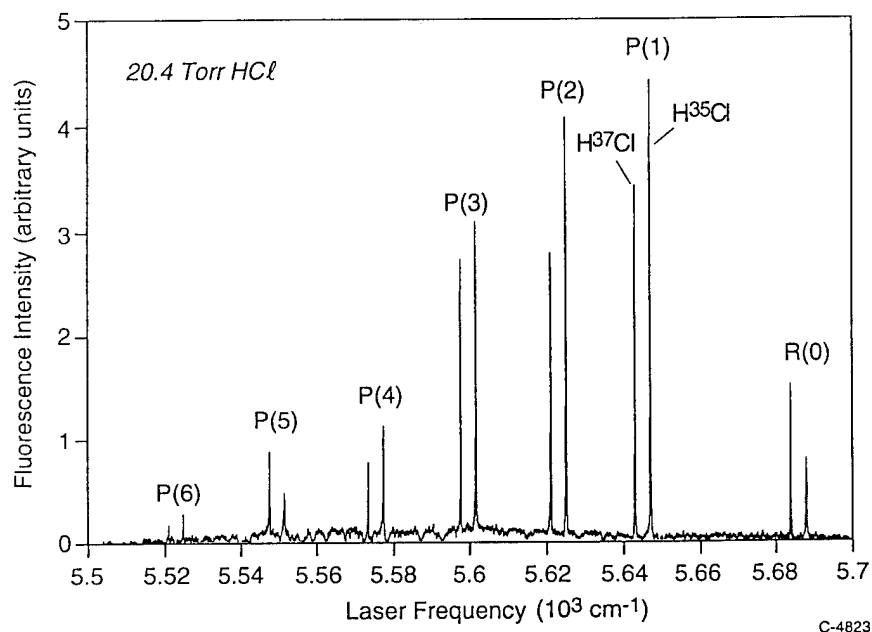


Figure 16
Excitation Spectrum of Several Lines in the (2,0) Band of HCl.
The Pairs of Lines Due to the Two Cl Isotopes are Indicated.

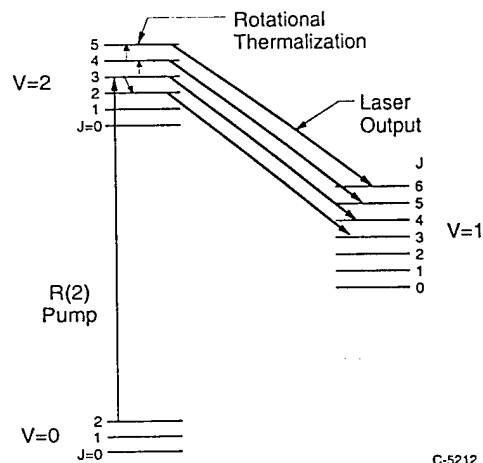
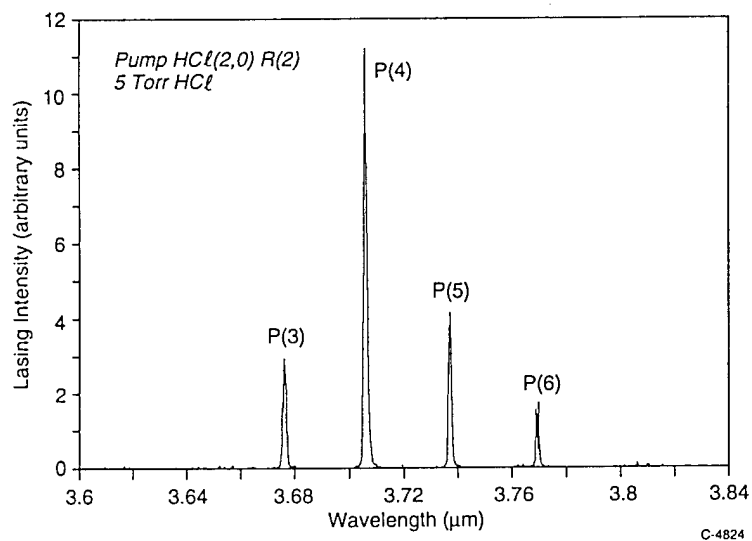


Figure 17
Spectrally Resolved HCl Laser Output Resulting from Excitation of the $J' = 2$ Level
Within $v' = 2$. The Relevant Energy Levels Are Also Indicated.

In summary, the HF and HCl laser experiments illustrate the nearly ideal laser properties of these species. For example, these species display high optical gains, lase over a wide range of cavity conditions, and produce high conversion efficiencies (quantum efficiencies of greater than 50%). These characteristics make the HX species strong contenders for development into mid IR lasers for Air Force applications.

6. ALEXANDRITE LASER PUMPED DF AND HCl LASERS

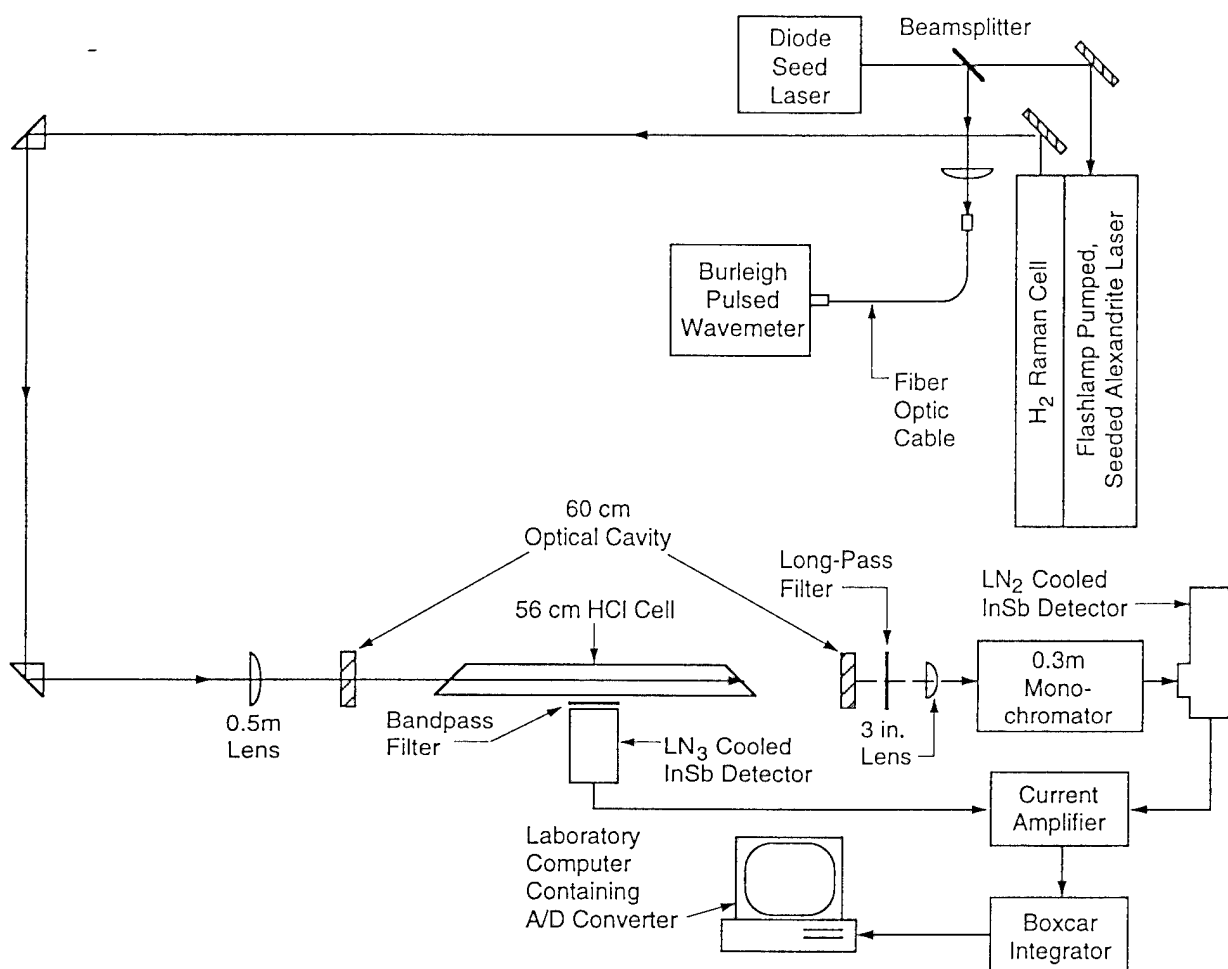
The experiments described above used relatively low power pump lasers to produce inversions and optically pumped lasers in HCl and HF. In order to extend these results to higher pump powers we have incorporated an alexandrite laser as the excitation source. The high power alexandrite laser can be Raman shifted to produce output appropriate for excitation on the (3,0) bands of several HX type molecules. We have performed two experiments to investigate this approach: a) a test at Light Age Inc. using one of their alexandrite lasers and b) tests at PSI with a high power alexandrite purchased under a Phillips Lab sponsored Phase II SBIR program. We discuss each of these experiments below.

6.1 DF Laser Experiments

We coordinated a two day test window with Light Age Inc., Somerset, NJ. We designed and constructed a portable gas handling system and laser cell that was transported to Light Age. We also brought all diagnostic instruments including IR detectors, a monochromator, and a lab PC. None of this experiment was available at Light Age. In order to meet the precise tuning and frequency control requirements of the alexandrite pump laser, the alexandrite oscillator was frequency locked with an AlGaAs diode laser operating near 790 nm. The alexandrite laser that Light Age made available had a ring cavity configuration. This device was being developed as a prototype for lidar applications. The diode laser seeder could only be used at wavelengths shorter than 790 nm and this limited the range of transitions that we could pump in DF. In addition, Light Age was experiencing alignment problems with the injection seeding the alexandrite ring cavity. Consequently, the laser was operating in a degraded condition.

The alexandrite laser was frequency locked with a single frequency AlGaAs diode laser that operated in the 785 to 790 nm range. Laser locking was obtained near 788.86 nm which when Raman shifted by a single Stokes shift in hydrogen, produced excitation near 1173 nm corresponding to the R(3) line of the (3,0) band in DF.

The DF laser demonstration tests were conducted using the apparatus shown in Figure 18. The DF was contained in a 56 cm long 2.5 cm diameter stainless steel cell. The MgF_2 end windows were attached at Brewster's angle. The cell also had a side viewing MgF_2 window to view laser induced fluorescence. The 60 cm long optical cavity consisted of a 3 m radius of curvature dichroic input mirror that was 60 to 80% transmissive at the 1.2 μm pump wavelength and 99.9% reflective at the 3.8 μm DF laser wavelength. The output coupler was 20% transmissive at the DF laser wavelengths. A cooled InSb detector was used to view side fluorescence and the DF laser output. We used a 0.3 m McPherson monochromator to spectrally resolve the DF laser output. The monochromator was equipped with a 300 groove/mm grating blazed at 2.1 μm . A Stanford Research Systems boxcar integrator and a lab PC were used to analyze both the fluorescence and laser output.



C-6028

Figure 18
Block Diagram of Alexandrite Pumped DF Laser

In Figure 19 we show an excitation scan of the DF R(3) line on the (3,0) band. The frequency tuning was accomplished by current tuning the 788 nm diode laser injection seeder. A spectrally resolved laser spectrum of DF(3,2) lasing is presented in Figure 20. For these data the alexandrite laser frequency was fixed at line center of the DF absorption. The signal to noise allowed definitive assignment of only a single laser transition at 3819.1 nm, corresponding to the P(5) line of the (3,2) band. For these data, the DF pressure was 40 Torr, and for the 56 cm cell, less than half of the pump beam was absorbed. We also observed amplified spontaneous emission, i.e., mirrorless lasing, demonstrating the high optical gains that we expect in DF.

6.2 Alexandrite Laser Pumped HCl Laser

A high energy alexandrite laser (Light Age PAL) was frequency locked with a single frequency AlGaAs diode laser that operated in the 790 to 795 nm range. Laser locking was obtained near 794 nm which when Raman shifted by a single Stokes shift in hydrogen, produced excitation

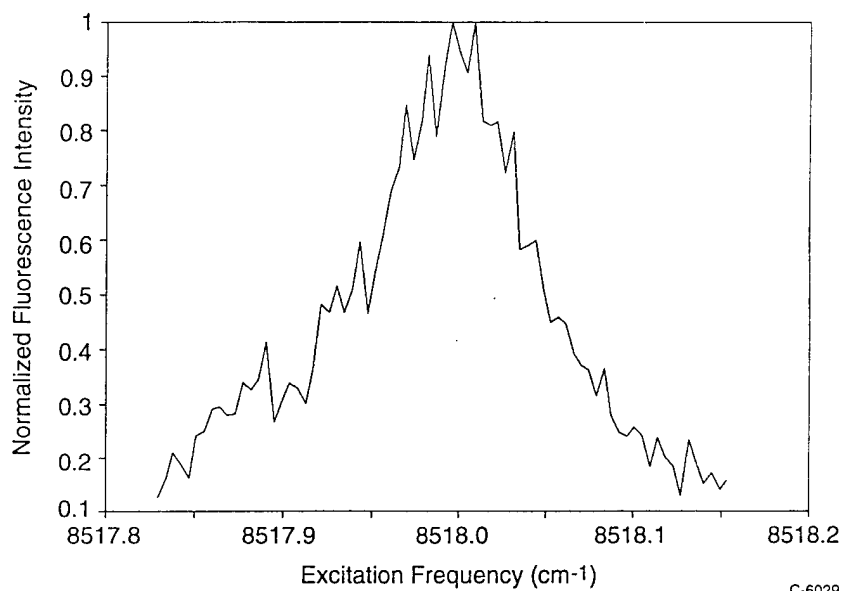


Figure 19
Laser Excitation Spectrum of the DF (3,0) Laser

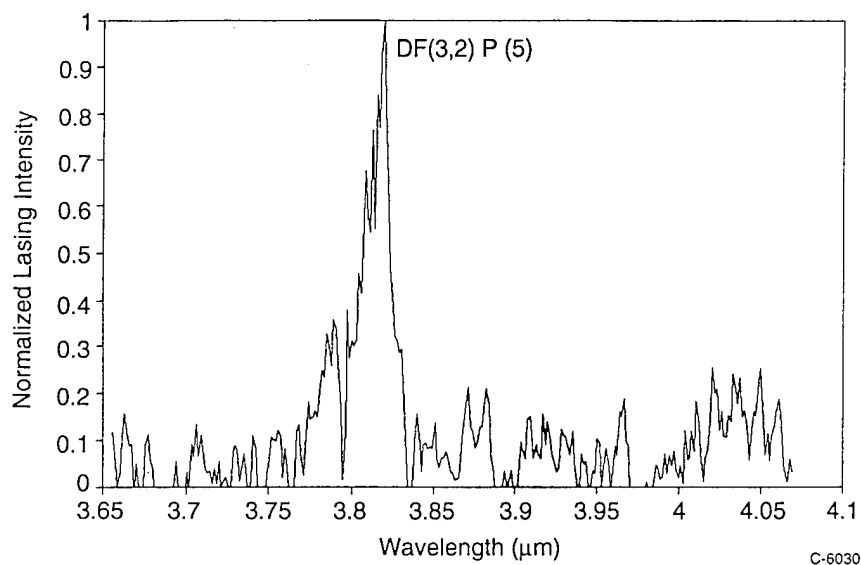


Figure 20
Spectrally Resolved DF Laser Emission From Alexandrite-Pumped DF Laser

near 1180 nm corresponding to absorptions on the (3,0) band in HCl. The injection seeding produces subdoppler emission from the alexandrite laser (500 MHz) that when Raman shifted can be used to pump overtone transitions in HCl.

The initial HCl tests were conducted using the apparatus similar to that shown in Figure 18. The HCl was contained in a 56 cm long 2.5 cm diameter stainless steel cell. The MgF_2 end windows were attached at Brewster's angle. The cell also had a side viewing MgF_2 window to view laser induced fluorescence. A cooled InSb detector was used to view side fluorescence and the DF laser output. Our initial tests consisted of scanning the wavelength of the diode laser injection seeder so that the Raman shifted output would scan a single HCl absorption line. The laser induced fluorescence from the pumped HCl was observed through the side window as described above. A typical trace is indicated in Figure 21. We performed this measurement as a function of the HCl concentration in the cell. By determining the full width at half maximum of each absorption trace we were able to obtain an initial estimate for the self broadening of the HCl (3,0) absorption line from the data shown in Figure 22. Our estimate for the broadening coefficient is 10 MHz/Torr. This value can now be used in the analytical model that has been developed to guide in the development of the HCl laser. The broadening coefficient is a crucial parameter in the efficiency of the absorption (pumping) process. The clear demonstration of the narrow band output of the diode laser, injection seeded alexandrite laser is also crucially important to the programs at Phillips Laboratory.

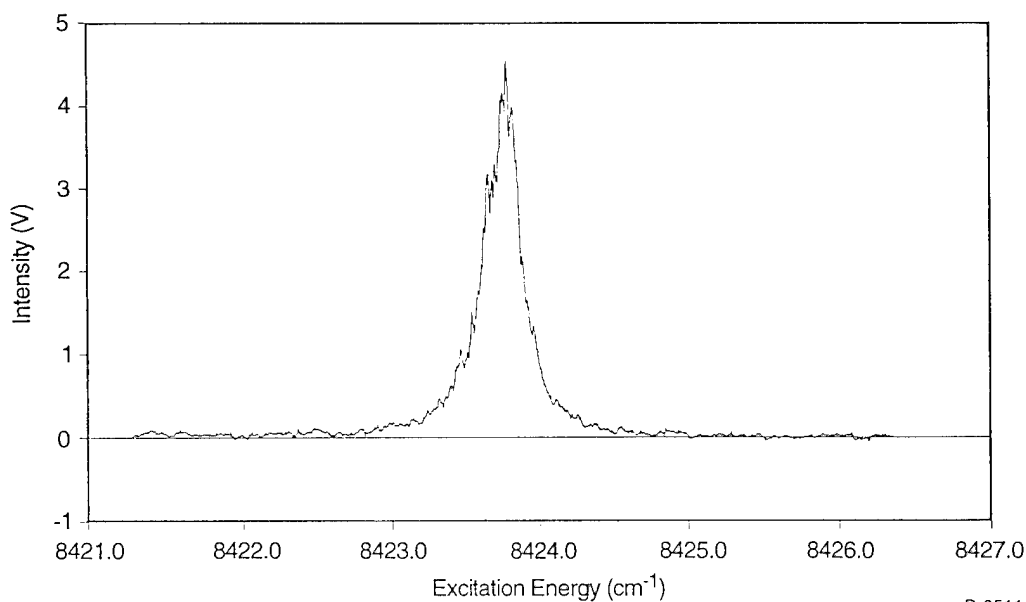


Figure 21

Laser Excitation Spectrum of HCl(J4) Line on the (3,0) Band Obtained
Using High Power, Narrow Band, Raman-Shifted Alexandrite Laser

Initial HCl laser experiments were completed using a 60 cm long optical cavity consisting of a 3 m radius of curvature dichroic input mirror that was 60 to 80% transmissive at the 1.2 μm pump wavelength and 99.9% reflective at the 3.8 μm HCl laser wavelength. The output coupler was 20%.

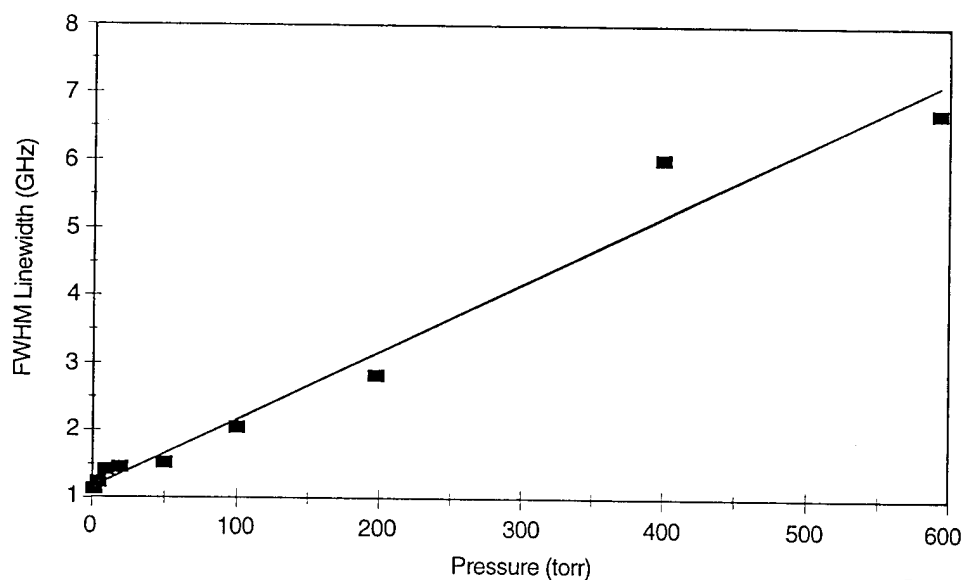


Figure 22

Linewidth of the LIF from HCl(J4) $v=3$ as a Function of the HCl Concentration

A Stanford Research Systems boxcar integrator and a lab PC were used to analyze both the fluorescence and laser output. We have observed HCl lasing from the initially pumped $v=3$ level, and preliminary data indicates cascade lasing on the (3,2), and (2,1) bands. This was a goal of the program and directly supports important applications at both WL and PL.

We point out that there may be some major advantages for pumping the (3,0) band in molecules such as DF. First, the weaker absorption can be used as an advantage since a double pass cell can lead to a more uniform gain medium when compared to the much stronger absorbing (2,0) band. Secondly, cascade lasing from the (3,2) and (2,1) bands can lead to much higher energy efficiencies and higher quantum efficiencies. Finally the (3,0) band absorption wavelengths for candidates such as HCl and DF can be reached using only a single Stokes shift, and this translates to higher pump powers.

7. DESIGN OF DIODE LASER PUMPED HF LASER

Production of mid-IR lasers pumped directly by a diode laser offers considerable promise for a compact and efficient system. However, as discussed in our last annual report, the kinetics of HX molecules is dominated by rotational and vibrational relaxation. Rotational relaxation does not present a problem since rotational thermalization within the vibrational level pumped by the excitation laser does not significantly affect the HX laser efficiency since the collisionally populated rotational levels can participate in the vibrational lasing process. However, vibrational relaxation can rapidly destroy the population inversion prior to radiative emission.⁵⁻⁷ This is not a serious issue for short pulse lasers (10 to 100 ns) since the excitation time scale competes favorably with the vibrational relaxation rates for nominal conditions. For long pulse or CW lasers such as diode lasers, vibrational relaxation becomes a severe constraint.

As we described earlier, we have concluded that under conditions where the HX molecules will efficiently absorb the diode laser pump radiation, the excited HX is rapidly quenched by collisions with the ground state HX reservoir. In brief, the kinetics are dominated by quenching. For example, in Figure 23 we show predictions of optical gain in DF pumped by a low power CW diode laser. The abscissa is the time from the onset of pumping. We observe that the gain is rather quickly quenched due to rapid vibrational relaxation. Thus, the laser would operate best in a pulsed mode. This could be accomplished by pulsing the diode laser or by rapidly tuning the diode laser through the molecular absorption band.

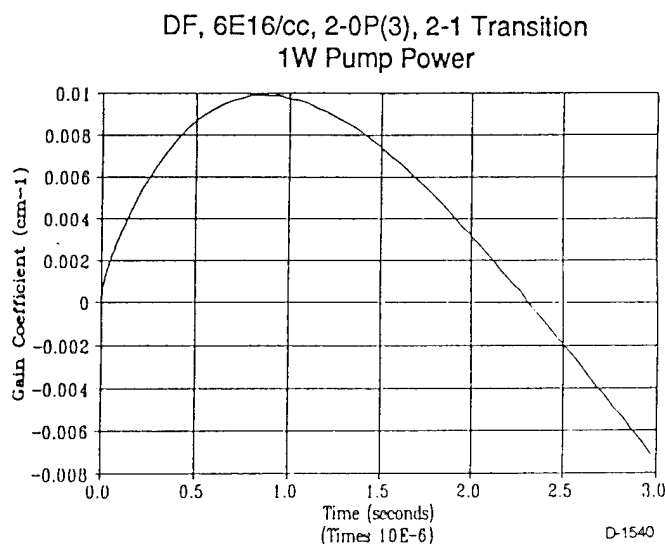


Figure 23
Predicted Optical Gain in DF for 1 Watt Pumped Power
and a DF Number Density of Approximately 2 Torr

Since it was clear that the kinetics of the HX vibrational relaxation dominate this pumping scheme, we considered two alternative approaches for developing an efficient laser pumped directly by diode lasers. The first involved flowing the HX gas similar to a CW dye laser. This

allows the HX molecules to be continually refreshed, and molecules that have already undergone the pump/laser cycle are swept from the cavity before a significant buildup of the terminal laser level. This scheme has been demonstrated in some of the early optical resonance transfer laser work on HF. For the present application, the HX would need to be flowed at nearly sonic speeds.

The second design, shows even greater promise. For a given laser excitation power, one can lower the HX quenching by reducing the HX number density in the laser cell. However, this will reduce the absorption coefficient and one will not efficiently couple the excitation radiation into the cell in a single or even double pass. This can be overcome by using resonant cavity pumping (RCP)^{8,9} as is currently done to efficiently frequency double low power CW solid state lasers and diode lasers. In RCP the optical cavity that contains the medium being pumped by the excitation laser is also a high Q cavity for the pump radiation. The intracavity intensity can be several hundred times greater than the pump laser itself. In effect the cavity is a Fabry-Perot interferometer tuned to be resonant with both the pump wavelength and the desired conversion wavelength. This configuration also requires that total round trip loss of the pump radiation by absorption be small ($\sim 1\%$), implying low HX pressures. Thus, the RCP offers much higher pump power and lower quenching. Preliminary modeling indicates that a direct diode pumped HX laser can be constructed using the RCP approach. For example, in Figure 24 we show the predicted gain of a RCP HF laser that uses a low power diode laser operating at $1.3\ \mu\text{m}$. The modeled conditions were: $[\text{HF}] = 1.5 \times 10^{15}\ \text{cm}^{-3}$, 50 cm cell length, and a circulating power of 143 mW. Single pass gains exceeding 10% are predicted. Furthermore, the gain lasts for over 100 μs . Clearly this approach has several advantages.

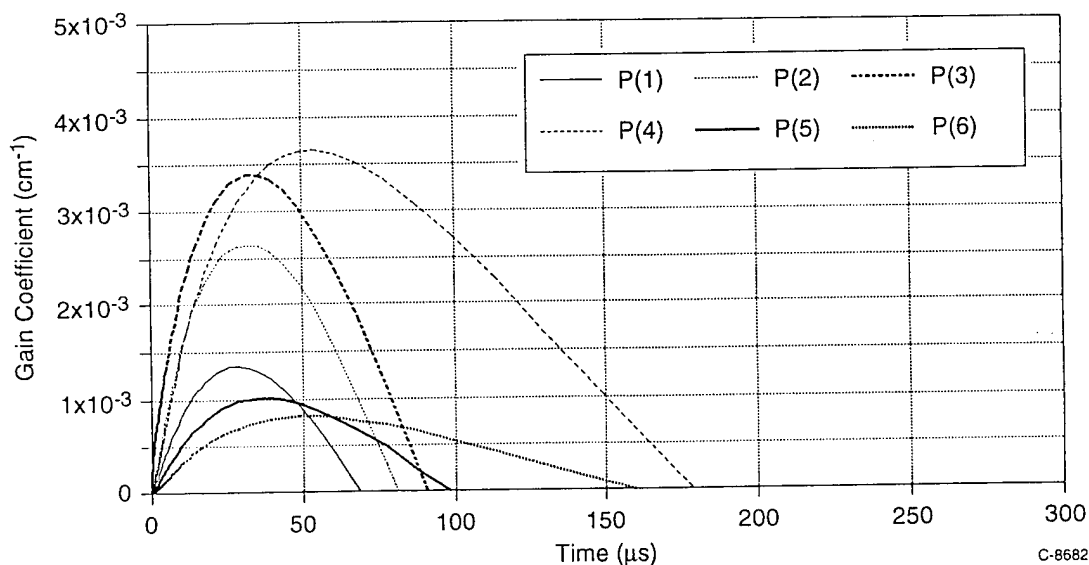


Figure 24

Predictions of Small Signal Gain Coefficient Using Resonant Cavity Pumping. For This Example We Assumed a Scattering Loss of 0.5%. Other Conditions Are Given in the Figure.

The major experimental challenge is to design and fabricate cavity mirrors that have high reflectivity at both the pump wavelength and the HX laser wavelength. We have mirrors that are provide some reflectivity at both 1.3 and 2.7 μm , the appropriate wavelengths for HF pumping on the (2,0) band with subsequent lasing on the (2,1) band. In a preliminary experiment we used a tunable diode laser to pump the HF(2,0) band while the HF cell was contained in an aligned cavity. The LIF from the (2,1) band was monitored using an InSb detector normal to the diode laser beam. As the diode laser was tuned over the absorption line there we observed enhancements in the LIF as the wavelength of the diode laser came into resonance with a cavity mode. Several of these appear on the LIF trace as shown in Figure 25. We feel that with mirrors of much higher reflectivities at both the pump and emission wavelengths an HF laser pumped by a miniature room temperature diode laser using this resonantly pumped cavity approach should be attempted.

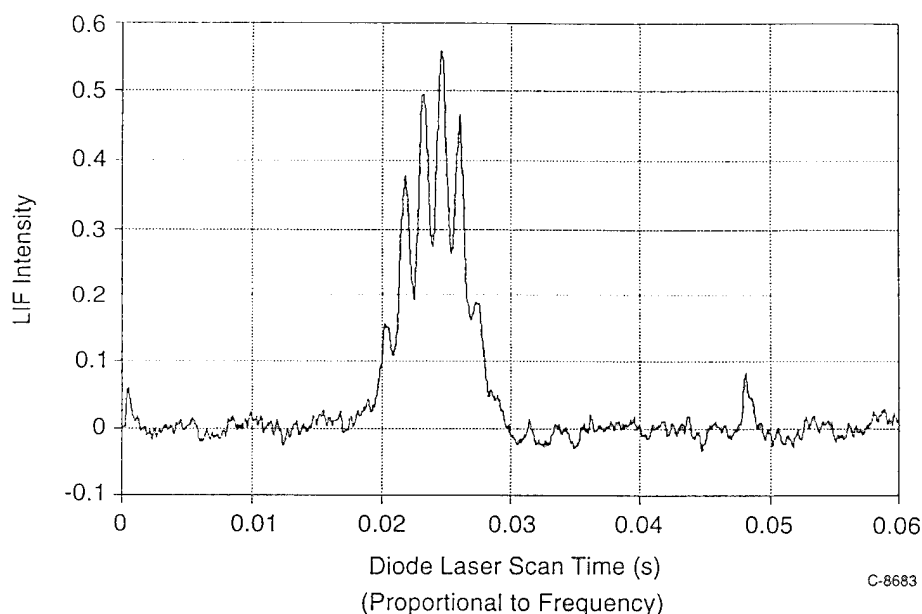


Figure 25
Laser Excitation Spectrum for HF(2,0) LIF as Diode Laser is Scanned Over the P Line.
The HF Cell Was Contained in an Aligned Optical Cavity.

8. APPLICATIONS OF DIODE LASER BASED SENSORS

Ultra-sensitive gas-phase detectors represent one of the most important applications of the room temperature diode lasers. Using common diode lasers that were developed for the communication industry we have demonstrated sensitive detection of several gases: H_2O , O_2 , NO_2 , HF , IF , I , and I_2 . The basic setup of these sensors is indicated in Figure 26.

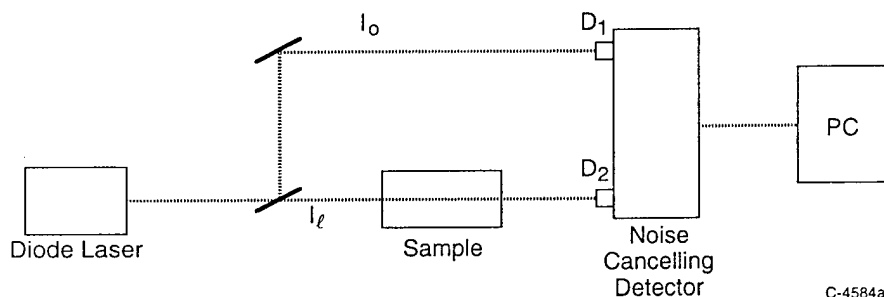


Figure 26
Layout for Typical Diode Laser Sensor

Typically we split the tunable diode laser output into two beams, one is a reference and the other is the sample or signal beam. Recently, we have been incorporating fiber optic delivery of the diode laser beams. We have found that fiber coupled lasers of a pigtailed configuration provide robust and easily maintained systems, and we have field tested several such units.

In practice, the diode laser frequency is tuned through a resonant absorption line of the species being probed, and the signals are recorded. Calibration curves of growth are recorded in order to quantify the absorptions. Depending on the strength of the absorptions we sometimes employ a balanced ratiometric detector (BRD) that allows accurate cancellation of laser excess noise that is carried on both the signal and reference beams. This device was originally developed for the communications industry.¹⁰ The BRD is used when small absorption ($< 1 \times 10^{-3}$) are to be measured. When the absorptions are on the order of a few percent, we simply use two independent detectors.

Regardless of approach, we scan the entire lineshape of the absorption feature. By integrating the recorded lineshape we can remove the temperature and pressure dependent broadening in the determination of the concentration of the species being measured. This can be valuable for many diagnostic applications. Alternatively, we can examine the recorded lineshapes to infer important parameters such as the translational temperature. As an example we present data recorded on atomic iodine. A heated quartz cell that contained molecular iodine was provided by the Phillips Lab. We heated the cell to several hundred degrees to dissociate a fraction of the iodine. The diode laser was used to probe the medium for atomic iodine. In Figure 27 we present absorption data that shows all 6 hyperfine components. A single scan took only 50 ms. In Figure 28 we show only the (3,4) line and a Gaussian fit to the data. The cell temperature determined with a thermocouple was 1050 K the temperature inferred from the fit was

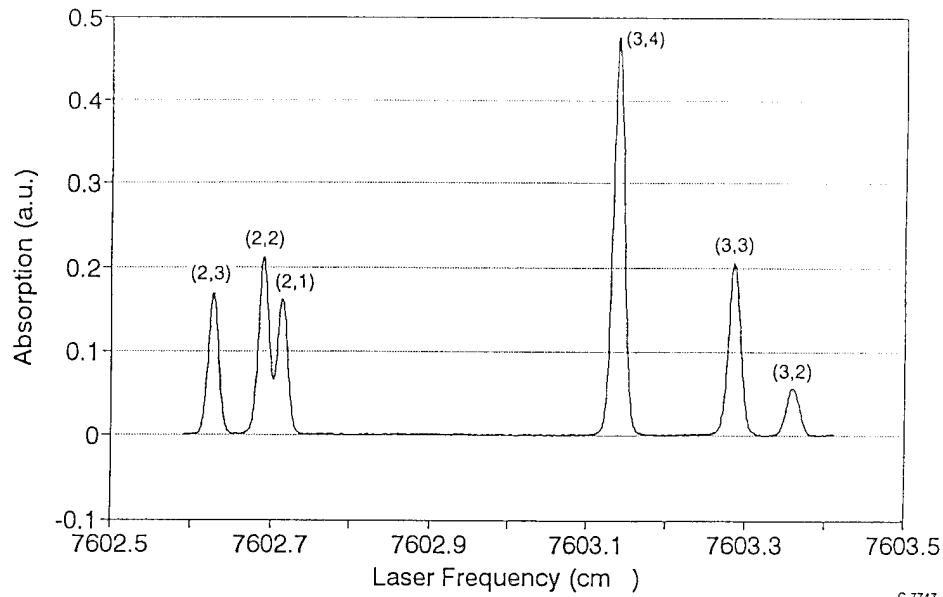


Figure 27
Absorption Spectrum of ($^2P_{1/2} - ^2P_{3/2}$) Line in Atomic Iodine Obtained at a Temperature of 1050 K. All Six Hyperfine Transitions Are Shown.

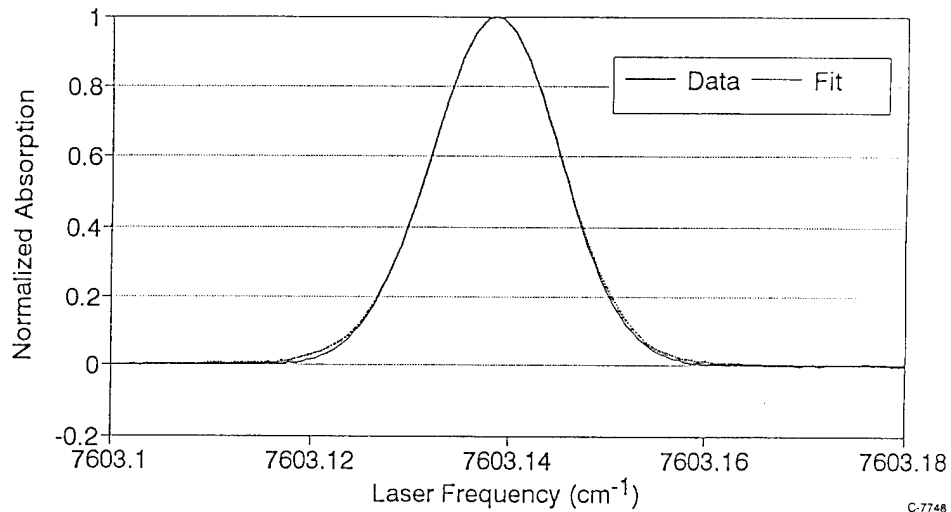


Figure 28
Absorption Spectrum of Atomic Iodine Near 1.315 μm Obtained With Tunable Diode Laser. Also Shown is a Comparison of a Gaussian Fit to the Data.

1000 K. Subsequent to these demonstrations we are developing an iodine diagnostic for COIL that will also be used to determine the temperature translational based on the I atom Doppler width.

8.1 Preliminary Determination of Linestrength of Water Absorption Line Near 1.39 μm

With the advent of tunable diode lasers, several groups have begun to use them as sensors for atmospheric gases such as O_2 , and H_2O . The HITRAN data base¹¹ is one of the most useful tools as a starting point for establishing a detection strategy for specific species. This comprehensive data base contains linestrengths, line positions in frequency or wavelength, and broadening coefficients. It has been common practice to use this data base to predict wavelengths required and to estimate ultimate detection sensitivities. However, we and others have^{12,13} found that reported linestrengths and line positions can be significantly in error when examined at the level of precision required for resonant absorption measurements, and this leads to inconsistencies in the sensor performance. Consequently, we have begun to make direct absorption measurements of the absorption strengths of some lines and then comparing them with the published HITRAN data base. In Figure 29 we present measured absorption on the 1392.3 nm water vapor absorption line as a function of water vapor concentration. The dark line is the prediction of HITRAN lowered by about 35% to match the data. Thus we found that the value in the HITRAN data base for this strong absorption line was in error. It is clear that additional measurements should be undertaken to improve the accuracy of this now widely used data base.

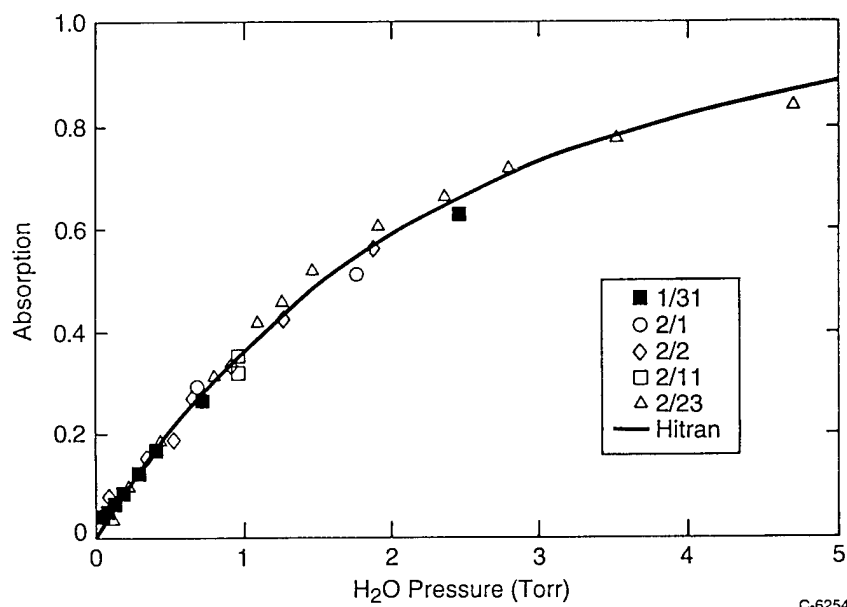


Figure 29
Curve of Growth for Water Vapor Absorption on the 1.39235 μm Line
vs Predictions of HITRAN

8.2 Water Vapor Sensor Development

Some initial experiments performed under support of this program have led to several sensors that have been developed and tested under separate funding. Indeed we have developed and delivered several complete monitoring systems to customers for the detection of water vapor. These include: Science Application International Corporation, a manufacturer of carbon-carbon composite materials, The Cloud and Aerosol Sciences Laboratory at the University of Missouri, Rolla, and The COIL Branch at the Phillips Laboratory, Kirtland AFB. We have been able to transfer this technology very rapidly. We have also demonstrated sensitive detection of both water vapor and oxygen in RADICL chemical oxygen iodine laser (COIL) at Phillips Laboratory. These diode laser based sensors provide non-intrusive, real time monitoring of these species that are crucial to the efficient operation of COIL. The current interest is aimed at improving the efficiency in order to reduce the COIL system weight for the ABL program.

We summarize some of the results obtained on RADICL in Figure 30 which shows water vapor concentration as a function of run time. Initially there is approximately 1 Torr of water vapor background from the oxygen generator. As the chlorine is added the temperature rises, and more water vapor is produced. Finally, the chlorine is shut off and the water vapor concentration drops. We are working closely with the Phillips Lab to interpret these and other data.

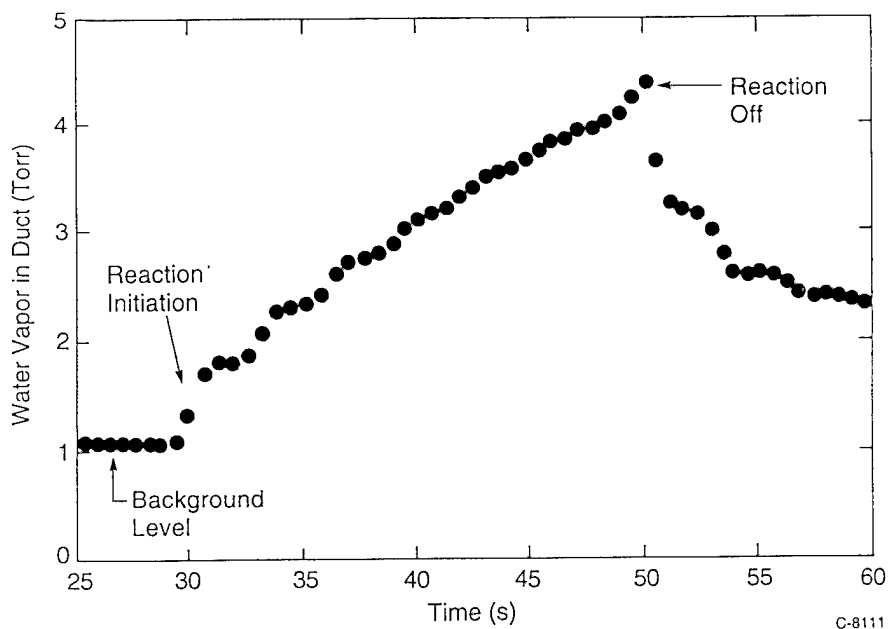
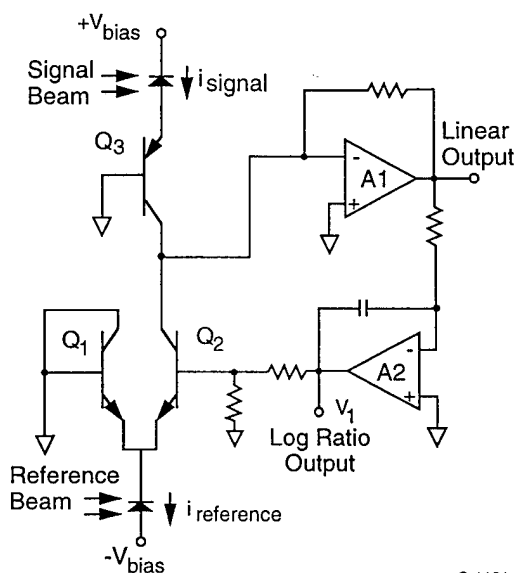


Figure 30
Evolution of Water Vapor From During a COIL Run

8.3 - Description of Ultra-Sensitive Absorption Measurements

Next we describe our efforts to develop an ultra-sensitive, two beam absorption technique. The balanced ratiometric detector (BRD) was originally developed by Hobbs¹⁰ for wavelength multiplexed communications applications, and shot noise limited absorbance measurements to 4×10^{-8} were reported on low pressure I_2 . We have modified and adapted it to be used by several lasers to detect numerous gas phase species. The basic features of the circuit are indicated in Figure 31. The essential feature of the BRD is that optical balancing of a conventional dual beam detection system is replaced with electronic cancellation of the two photodetector currents. The key is that intensity fluctuations in the diode laser output present in both the signal and reference beams can be coherently canceled. Since Si and InGaAs photodetectors exhibit wide dynamic range linearity, coherent photocurrent balancing is possible over a very wide frequency band. Noise cancellation is achieved by balancing the photocurrents at the summing junction of A_1 . The integrating feedback amplifier A_2 is used to maintain this balance by sensing the output of A_1 and adjusting the base emitter voltage of Q_2 .



C-1181

Figure 31
Schematic of Balanced Ratiometric Detector System

One of the attractive features of the BRD is that the output V_1 is given by

$$V_1 = G \ln[(I_{ref}/I_{sig}) - 1] \quad (2)$$

where G is the gain of A_2 . Substituting Beer's law for the ratio I_{ref}/I_{sig} we derive the relationship between the measured voltage and the laser absorbance, α

$$V_1 = G \ln[\exp^{\alpha} - 1] \quad (3)$$

This provides a convenient method for measuring absorptions.

8.4 Development and Testing of Diode Oxygen Sensor for COIL

One of the most important parameters in the COIL laser is the concentration of singlet delta oxygen. To date this has been determined in COIL by observing the (a-X) emission from O_2 with a Ge detector. While relatively simple to incorporate such as system, the absolute photometric calibrations required to interpret the data are difficult, and the accuracy of the technique is probably only $\pm 30\%$. This is insufficient for the design of upgraded COIL devices. Consequently, we have been developing a diode laser based device that measures the concentration of ground state oxygen by resonant absorption on the (b <- X) system near 760 nm. A room temperature diode laser is tuned through selected rovibronic transitions and the absorption trace is integrated to yield the oxygen concentration using the known linestrength of the b <- X transition. Knowledge of the oxygen ground state concentration can be used to calculate the singlet delta concentration from the following considerations. The reaction of molecular chlorine with basic hydrogen peroxide is known to yield oxygen as a product. One Cl_2 molecule yields one O_2 . All the O_2 is produced in either the $a^1\Delta$ or the $X^3\Sigma$ state; the crucial question is the percentage of [a]/[X]. Since each Cl_2 produces one O_2 , we can calculate the [a] if we know the chlorine flow rate and the concentration of ground state O_2 . The Cl_2 flow rate is measured using mass flow meters, so our measurement of $[O_2(X)]$ can be used to calculate $[O_2(a)]$.

The diode laser frequency is scanned across an individual absorption line at high rates (100 to 1000 Hz). This allows rapid signal averaging of complete absorption waveforms from which the concentration is determined. By integrating the recorded lineshape we can remove the temperature and pressure dependent broadening in the determination of the concentration of the species being measured.

Field tests were performed using the oxygen sensor at the RADICL COIL device at the Phillips Laboratory at Kirtland AFB. We used a fiber coupled laser to introduce the diode laser sample beam into the gain region of the COIL device. The weak absorption of the (b <- X) transition in oxygen forced use to also incorporate a multipass Herriot cell into the gain region. Our initial tests were very encouraging. We were able to observe the absorption lines from chemically produced oxygen, and we were able to calculate the number density of the oxygen produced. Of particular interest was the observation of an increase in the ground state oxygen concentration when molecular iodine was added to the COIL nozzle. This increase was due to the consumption of singlet delta oxygen by the dissociation of the I_2 . This real time observation of singlet delta consumption will be extremely useful in a more thorough understanding of operation of supersonic COIL devices and will be valuable in the design of efficient, advanced COIL devices.

In Figure 32, we present typical traces of oxygen absorption spectra obtained using our sensor. We show the (b<-X) absorption both in the absence and presence of I_2 . In Figure 32 the "hot flow 6" was obtained with I_2 being injected, and we observe the increase in the absorption from the $O_2(X)$ state due to the consumption of $O_2(a)$ state by the iodine dissociation. These data are

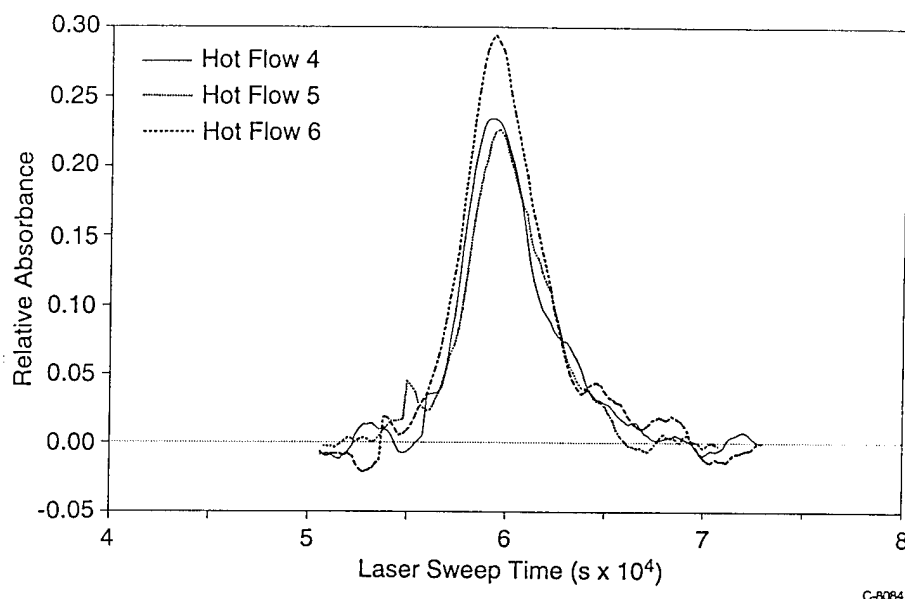


Figure 32

Data from RADICL Test at Phillips Lab. "Hot Flows" 4 and 5 Show Absorption Traces of Oxygen ($b-X$) Without Iodine Added. In "Hot Flow" 6, Molecular Iodine Had Been Added to the Flow and Production of $O_2(X)$ via Consumption of $O_2(a)$ During Dissociation is Evident.

supplying important anchors for analytical models that have been developed for the COIL devices. This diagnostic will be crucial for the development of advanced COIL generators and lasers. Additional data has been recorded from an improved O_2 sensor and is currently being analyzed.

8.5 Demonstration of Gain on the I_2 ($B \rightarrow X$) System Produced By a Low Power Diode Laser

With the advent of higher power diode lasers there has been considerable recent interest in using these efficient, miniature devices as excitation sources for a variety of lasers. Diode laser pumped solid state lasers have made impressive progress. Numerous commercial systems are now available. Efficient non-linear frequency conversion has also allowed these miniature diode pumped systems to operate over extended wavelength ranges. For example, commercial systems that produce the second, third, and fourth harmonics of Nd:YAG fundamental are also available. Indeed, efficient pumping of solid state lasers was one of the primary motivations for the development of high power diode lasers.

While the recent literature is rich with reports of diode laser pumped solid state lasers, there has been very little work reported in pumping gas phase species with diode lasers. We have been investigating the possibility of producing efficient gas phase lasers using miniature diode lasers as the pump source. In this report we describe preliminary results in which a 630 nm diode laser was used to produce a population inversion between levels of the B and X states in molecular iodine. We briefly describe the experiments and the initial results. This system serves as a prototype for other possible laser systems.

8.6 Experiment

The experiment consisted of using a 630 nm diode laser as the excitation source for the molecular iodine. The diode laser was operated at a frequency of 15811.45 cm^{-1} . The diode laser operated on a single longitudinal mode, and the output frequency was measured with a Burleigh WV 20 Wavemeter. Iodine crystals were contained in a 10 cm long cell. At room temperature the iodine vapor pressure is approximately 300 mTorr. All experiments were run at room temperature. The experimental setup is indicated in Figure 33.

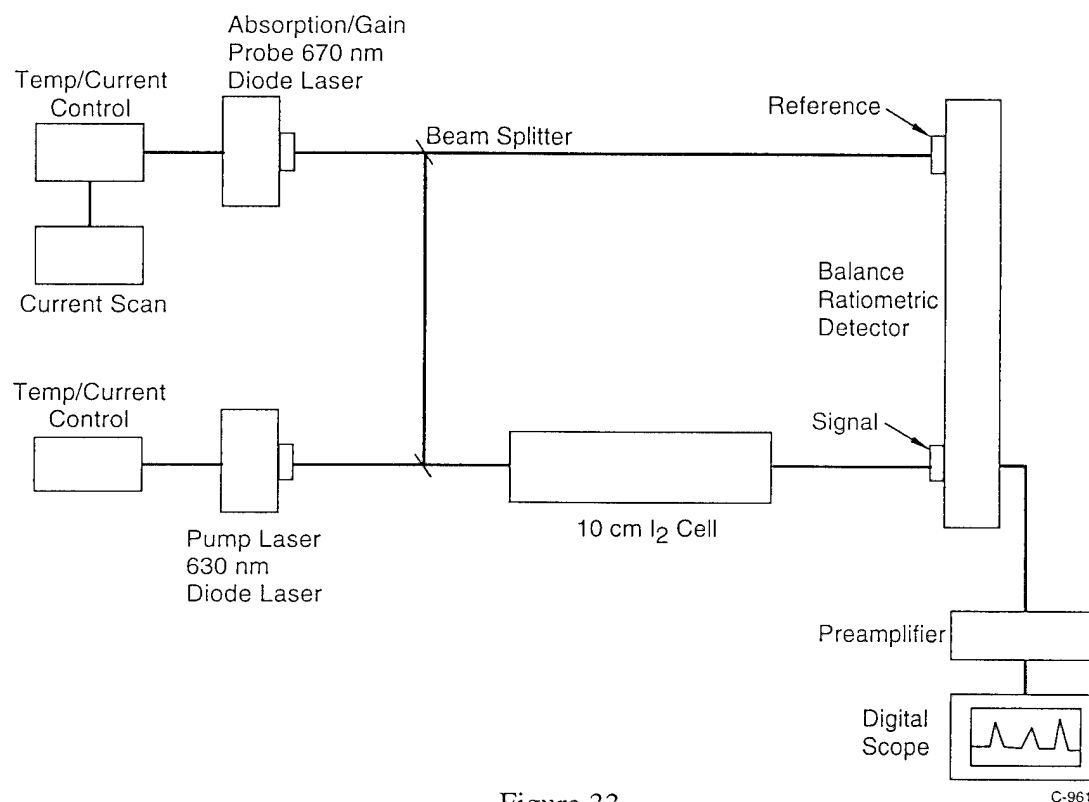


Figure 33

Experimental Arrangement for Demonstration of Pumping of $\text{I}_2(\text{B})$ by a Low Power Diode Laser

The second diode laser (Phillips CQ 806) was current scanned over a region near at 14783 cm^{-1} in order to probe the P(38) and R(46) lines of the (8,9) band. Although this was not the optimum gain level, it provided a region attainable with conventional diode lasers. In addition any absorptions from nearby lines can be used to calibrate any gain that is observed.

The 630 nm diode laser pumped two rotational transitions within the B-X (8,4) band: P(38) and R(46). Doppler broadening effectively blends the transitions. From the measured absorption of the pump beam (approximately 10%) we expect that the steady state number density in $v'=8$ will be $\leq 2 \times 10^9 \text{ cm}^{-3}$ for a pump power of 10 mW incident on the cell with a 0.5 mm beam diameter. The experiment consisted of fixing the pump laser on the (8,4) band and probing for gain on the (8,9) band. Calculations and modeling completed prior to the experiment had

indicated that we might be able to produce gains on the order of a tens of ppm/cm. Thus we incorporated our balanced ratiometric detector (BRD) that we have been developing to allow ultra-sensitive loss measurements to be made on gas phase species. The detector allows coherent noise cancellation in a two beam absorption measurement (I_{ref} and I_{sig}). Using this detector we have been able to measure absorptions close to the shot noise limit for low power diode laser beams.

The probe laser was scanned over a spectral region of approximately 0.2 cm^{-1} . This encompassed both the P(38) and R(46) lines in the (8,9) band. The pump/probe scheme is shown in Figure 34. Only one branch is indicated to simplify the figure. When the probe diode laser was scanned with the pump laser off resonance and not pumping the (8,4) band we observed weak absorption peaks as indicated in Figure 35. We have assigned these lines as the P(38) and R(46) absorption lines on the (8,9) band. The detector is allowing us to observe absorptions from $v''=9$ in $I_2(X)$. The relative vibrational population is reduced by a factor of approximately 10^4 from that in $v''=0$. This provides not only a good example of the sensitivity of the detection system, but also provides a solid calibration for gains and or losses since the absorption on the (8,9) band can be accurately calculated. Our detector is linear in absorption for these small values.

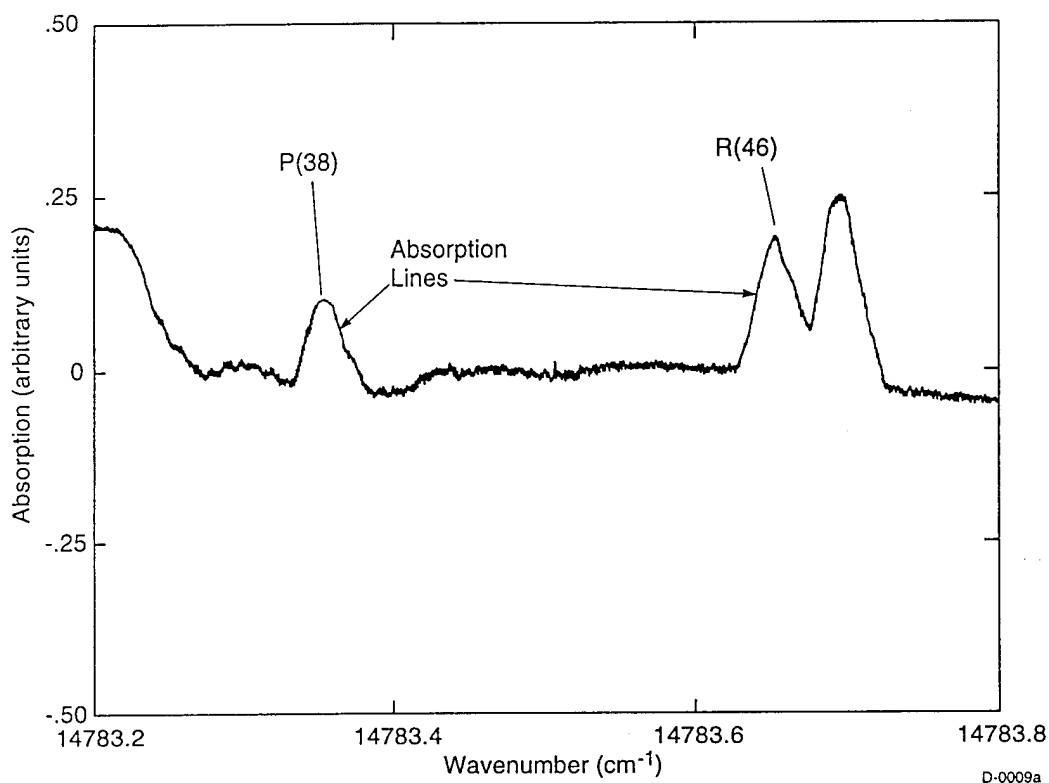


Figure 34
Absorption From Ground State Iodine. Transitions Are Indicated.

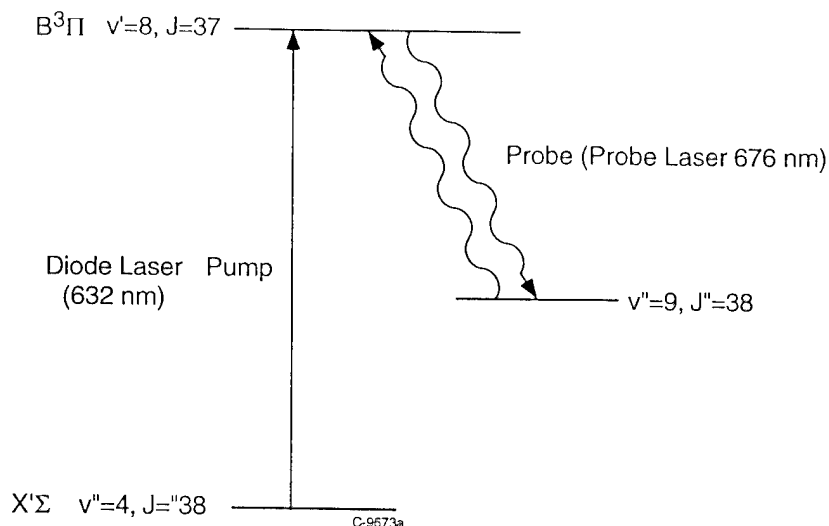
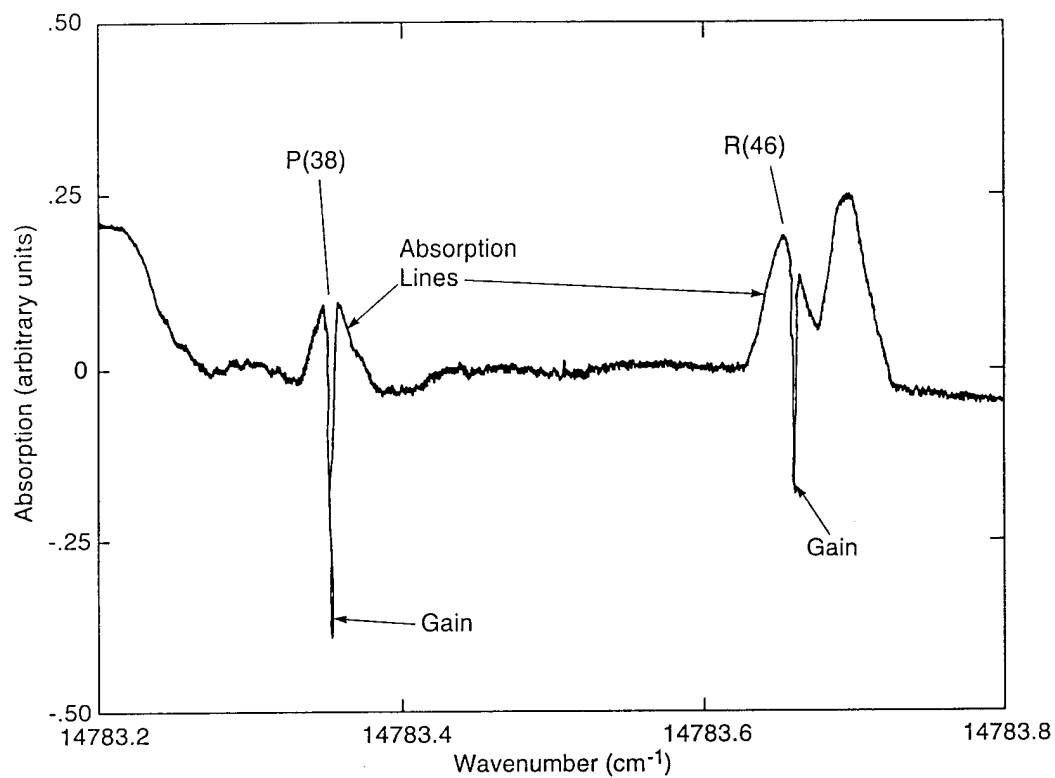


Figure 35
Pump/Probe Scheme Used in This Experiment

When the pump laser is tuned to pump the (8,4) band, bright visual laser induced fluorescence is observed in the cell. In addition the absorption trace changes dramatically as shown in Figure 36. The absorption lines now have sharp gain features on them. We are examining these data and offer the following preliminary interpretation. The diode laser pump is operated single longitudinal mode and is expected to have a bandwidth of less than 50 MHz. Thus the pump excites only a small velocity group from the Doppler profile. This small velocity group is deposited in $v'=8$ of $I_2(B)$. There it can undergo collisions of several kinds including: momentum exchange, rotational transfer, vibrational transfer, and electronic quenching. In addition, some spontaneous predissociation and spontaneous emission occur. The probe laser since it is sweeping in frequency undergoes absorption from the (8,9) band until it reaches the frequency of emission from the small velocity group that is excited in $v'=8$. For this narrow range the probe laser is amplified as indicated by the switch in sign of the absorption trace.

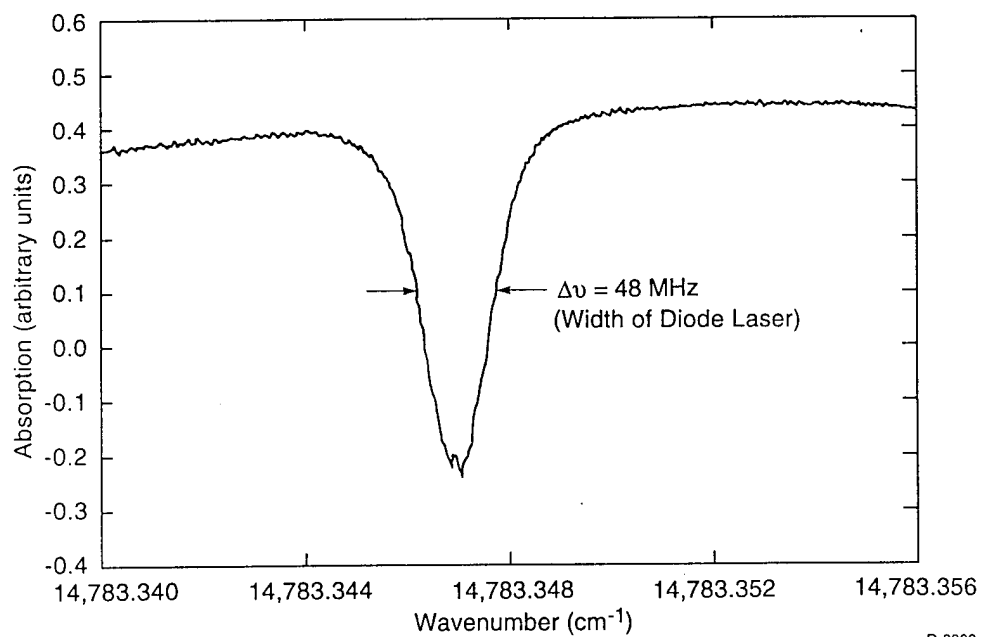
An expanded view of the P(38) line (Figure 37) shows that the width of the gain line is approximately 50 MHz, consistent with the narrow pump laser. The magnitude of the measured gain is approximately $2 \times 10^{-4} \text{ cm}^{-1}$. This is consistent with the calculations that we completed prior to initiating the experiments. We have observed gain for pump powers as low as 200 μW .

These results confirm that diode lasers are viable as miniature, efficient pump sources for gas phase laser candidates. It should be possible to demonstrate lasing on iodine with our present setup. These concepts should be extendable to other molecules including those that provide lasing from 600 to 4500 nm. The incorporation of diode lasers as efficient pump sources for gas phase lasers was an important goal of our effort. This demonstration was crucial to proving this concept. This ultra-sensitive gain technique may have some significant spectroscopic applications since it provides a convenient sub-doppler method for probing atoms and molecules.



D-0009

Figure 36
Diode Laser Scan Showing Gain Produced Over Narrow Frequency Interval



D-0008

Figure 37
Expanded View of the P(38) Line Showing Gain
Within the Doppler Width of the Absorption Transition

9. CONCLUSIONS

In this report we have provided results of a comprehensive study of the production and application of near- to mid-IR lasers. Several excitation strategies and sources for excitation of both electronic transition and vibrational lasers have been discussed. Specific examples include: a miniature Nd:YAG pumped I₂ laser and HF, DF, and HCl lasers. These devices provide output wavelengths from 700 nm to nearly 4000 nm. The hydrogen halide systems are efficient and show promise for development into higher power devices.

We have also developed several gas phase sensors using near IR diode lasers. These devices will not only be valuable as environmental sensors, but also for process control and as spectroscopic and kinetic tools for basic research. In an early transfer of this technology, we have developed and tested O₂, I, and H₂O sensors for the COIL laser. These devices will be valuable not only for health monitoring of the COIL laser but the data produced will facilitate the design of high power devices.

Finally, we have demonstrated an ultra-sensitive gain/loss diagnostic applicable to new and existing laser systems. This device was tested using a low power diode laser to produce small gains ($\approx 10^{-5} \text{ cm}^{-1}$) in molecular iodine. This diagnostic not only allows the magnitude of the gain to be determined, but also provides valuable information such as the spectral width of the gain feature. Sub-doppler gain profiles were readily recorded. The gain/loss diagnostic will be further applied in future programs.

10. REFERENCES

1. Davis, S.J., Hanco, L., and Wolf, P.J., *J. Chem. Phys.* **82**, 4830 (1985).
2. Koffend, J. Brooke and Field, Robert W., *J. Appl. Phys.* **48**, 4468 (1977).
3. Kroll, M. and Innes, K.K., *J. Mol. Spectrosc.* **36**, 295 (1970).
4. Glessner, J.W. and Davis, S.J., *J. Appl. Phys.* **62**, 1 (1987).
5. Oba, D., Agrawalla, B.S., and Setser, D.W., *JQSRT* **34**, 282 (1983).
6. Copeland, R.A. and Crim, F.F., *J. Chem. Phys.* **78**, 5551 (1993).
7. Dzelzkalns, L.S. and Kaufman, F., *J. Chem. Phys.* **79**, 3363 (1983).
8. Dixon, G.L., Tanner, Carol E., and Wieman, Carl E., *Optics Lett.* **14**, 731 (1989).
9. Kean, P.N. and Dixon, G.J., *Optics Lett.* **17**, 127 (1992).
10. P.C.D. Hobbs, "Shot noise limited optical measurements at baseband with noisy lasers," *Laser Noise*, SPIE Volume 1376, 216 (1990).
11. L.S. Rothman, R.R. Gamache, A. Goldman, L.R. Brown, R.A. Toth, H.M. Pickett, R.L. Poynter, J.-M. Flaud, C. Camy-Peyret, A. Barbe, N. Husson, C.P. Rinsland, and M.A.H. Smith, "The HITRAN database: 1986 edition," *App. Opt.* **26**, 4058 (1987).
12. S. Langlois, T.P. Birbeck, and R.K. Hanson, "Diode Laser Measurements of H₂O Line Intensities and Self-Broadening Coefficients in the 1.4- μ m Region", *J. Molecular Spectroscopy*, **163**, 27 (1994).
13. S.L. Bragg, S.A. Lawton, and C.E. Wiswall, "Absolute measurements of absorption at the iodine-laser frequency in atmospheric gases", *Optics Lett.*, **10**, 321 (1985).